



48 1. Introduction

49

50 The Earth's stratospheric aerosols mainly contain liquid particles as pure mixture of
51 water and sulfuric acid particles (hereafter referred to as sulfate aerosols or sulfate
52 particles). They largely originate from natural and anthropogenic emissions of oxidized
53 carbonyl sulfide (e.g. Kremser et al., 2016; Günther et al., 2018) or are released from
54 volcanic eruptions injecting the SO₂ aerosol precursor directly into the stratosphere (Russell
55 et al., 1996; Deshler et al., 2003; Solomon et al., 2011; Jégou et al., 2013; Bègue et al., 2017),
56 with an altitude of injection controlled by the eruption intensity. Aerosols from volcanic
57 eruptions of moderate amplitude (i.e. about 20 times less SO₂ injected than for the Pinatubo
58 major volcanic eruption in 1991) occurring regularly since the year 2000, modulate the
59 sulfate aerosol concentration at the global or hemispherical scale over periods of months
60 (Vernier et al., 2011). Nevertheless, observations of the aerosol content show that particles
61 concentration remains presently low in the northern hemisphere stratosphere, as compared
62 to the post-1991 period impacted by the Pinatubo volcanic eruption. Hence, in what follows,
63 the current stratospheric conditions are typically referred to as "background" aerosol
64 conditions, with sulfate particle concentrations expected to decrease with increasing
65 altitude above 20 km (Deshler et al., 2006).

66 Although sulfate particles are the main component of the stratospheric aerosols, at
67 least in the lower and middle stratosphere, remote sensing and in-situ measurements
68 performed for more than 30 years have shown that materials (not considering frozen
69 material) clearly stand out from the sulfate population in terms of composition and optical
70 properties, with abundances depending on the altitude, latitude, and season (Baumgardner
71 et al., 2004; Curtius et al., 2005; Murphy et al., 2007; Renard et al., 2008; Ebert et al., 2016;
72 Schütze et al., 2017). Such materials, that we define here as NSPs, acronym for "Non-pure
73 Sulfate Particles", could be externally-mixed (i.e. pure solid and liquid particles) or internally-
74 mixed (i.e. included in or coated by pure sulfate). This definition clusters the various complex
75 properties, mainly in terms of composition, shape and conditions of sublimation, reported in
76 the literature. NSPs can be in the form of semi-volatile particles like some secondary organic
77 aerosols, or volatile liquid particles formed from gaseous precursors, with or without
78 dissolved material. They can contain refractory or non-refractory material in the form of
79 amorphous, compact, aggregated or fractal solid parts like black carbon, thereafter BC, or
80 soot particles (black carbon refer to pure carbon particles, while soot are carbonaceous
81 particles including carbon and other materials). These particles are mostly optically-
82 absorbing conversely to pure sulfate particles.

83 NSPs can have different origins, coming either from the Earth or from space. As
84 detailed below, the strong variability in the corresponding concentration and chemical
85 composition measurements could be due to the various sources, including possible very
86 localized contributions. The expected low concentrations of these particles, the wide variety
87 of their shape and their chemical compositions and the various sensitivity of the
88 measurement techniques have not, up to now, made it possible to reach a comprehensive
89 vision of non-sulfate materials in the stratosphere in terms of origins, content, physical
90 properties, composition and seasonal/inter-annual variability, which would be necessary to
91 address different questions such as radiative effects.

92 The aim of this paper is to contribute to a better understanding of NSPs origins and
93 variability in the stratosphere. For that purpose, we have developed a new strategy of
94 measurements, using the Light Optical Aerosols Counter (LOAC), which has performed 135



95 flights under weather balloons over the mid-2013 – mid-2019 period. We first present the
96 methodologies already used for the NSPs detection; then, we present the LOAC instrument
97 and the results obtained for concentrations, size distribution, temporal and spatial
98 variabilities; finally we discuss the possible origins of such variabilities, and the contribution
99 of LOAC to better estimate the source of the NSPs.

100
101

102 **2. Present methodologies for NSPs detection in the stratosphere**

103

104 **2.1 Context**

105

106 NSPs have been detected using different remote-sensing and in-situ instruments,
107 from the ground, onboard airplanes, under balloons and onboard satellites. None of these
108 instruments can solely characterize these particles at all possible scales, from the detection
109 of specific events to the observation of the spatial and temporal variability of their
110 concentrations, size distributions and chemical composition. Then, all these measurements
111 must be combined to tentatively propose a comprehensive view of NSPs in the stratosphere.

112

113

114 **2.2 Ground-based measurements**

115

116 Ground-based observations provide sparse or time-series measurements from a
117 given place, meaning that fortuitous events of stratospheric aerosol enhancements with or
118 without NSPs can be detected.

119 Remote-sensing photometric measurements at twilight can provide vertical profiles
120 of twilight intensity that reflect the aerosol abundances. However, such measurements have
121 been seldom conducted, mainly during meteor shower episodes, showing strong and
122 transient aerosols enhancements in the middle and upper stratosphere (Padma Kumari et
123 al., 2005, 2008).

124 Other transient episodes have been reported from lidar measurements, in relation
125 with the disintegration of a meteorite (Klekociuk et al. 2005), or the debris of rockets or
126 satellites (Gerding et al., 2003), or wildfire plume events (Siebert et al., 2000; Khaykin et al.,
127 2018; Haarig et al., 2018). Most of these measurements are performed in the framework of
128 the Network for the Detection of Atmospheric Composition Change (NDACC) or European
129 Aerosol Research Lidar Network (SEARLINET). There is however no direct determination of
130 the precise size distribution and concentration of the particles, although indications on the
131 altitude dependency of their nature (liquid, solid, mixed) and their mean size values can be
132 derived from the depolarization they induce on the backscattered laser light (Stein et al.,
133 1994). Such analyses are conducted from an optical point of view by partitioning the
134 stratospheric aerosol into icy particles and spherical particles containing sulfate component,
135 which backscatter light is well-known, and non-sulfate optical component that mainly refers
136 to light-absorbing material including BC and soot. In particular, such a partitioning was
137 already performed by Miffre et al. (2015) in the troposphere when coupling incandescence
138 and lidar field measurements.

139

140

141



142 **2.3 Airplane measurements**

143

144 Airplanes can perform long horizontal excursions but shorter vertical profiles
145 excursions in the lower stratosphere up to about 22km altitude, by carrying instruments for
146 in-situ measurements. The measurements are conducted during dedicated field campaigns,
147 thus providing accurate but sparse measurements that might not be representative of the
148 whole lower stratosphere. The main difficulty could be the collection of very large particles
149 greater than several tens of μm , although specific collecting methods have been developed
150 to limit the possible breaking of the particles due to relative speeds of up to 200 m/s (e. g.
151 Scott and Chittenden, 2002).

152 Historically, the first campaigns were conducted to collect interplanetary dust, with
153 subsequent laboratory analysis by electronic microscopy (TEM/SEM) and energy-dispersive
154 X-ray microanalysis (Brownlee, 1985; Warren and Zolensky, 1996). NASA has been collecting
155 dust in the stratosphere since the beginning of 1981, with U-2, ER-2 and WB-57 airplanes.
156 These flights have mostly ranged over most of the USA (as far as north as Alaska) and Central
157 America. The main challenging tasks are to distinguish between the refractory material
158 coming either from space or from the Earth itself and to determine the natural or
159 anthropogenic origin of these particles through morphology and composition analyzes
160 (Pueschel et al., 1992; Blake and Kato, 1995; Pueschel et al., 1997; Strawa et al., 1999; Ebert
161 et al., 2016; Schütze et al., 2017).

162 In-situ optical counting instruments onboard airplanes provide the size distribution of
163 the particles in the lower stratosphere, for particles greater than about 0.2 μm . Conventional
164 counters are highly sensitive to the complex refractive index of the particles; BC particles can
165 typically be up to 10 times darker than liquid sulfuric-acid aerosols of the same size. To
166 accurately retrieve the size distribution, the nature of the detected aerosols must be known
167 when processing the data, otherwise the contribution of the optically-absorbing particles
168 could be strongly underestimated. A more sophisticated methodology consists in using a first
169 channel specifically for the determination of the total aerosol concentration and a second
170 one heated to 250°C detecting the presence of non-volatile materials. The fraction of
171 stratospheric particles not composed entirely of volatile (i.e. water and sulfuric acid)
172 material is then estimated by calculating the difference between both channels (Curtius et
173 al., 2005).

174 The in-situ scattering and incandescence techniques, where the aerosols are also
175 heated, is used to determine the size distribution of the submicron particles down to 0.2 μm ,
176 the proportion of light-absorbing refractory NSPs, the determination of bulk composition
177 (such a BC) and information about the possible presence of coating (Baumgardner et al.,
178 2004; Schwarz et al., 2006; Weigel et al., 2014).

179 Finally, the in-situ mass spectrometry provides the composition of the particles and
180 the vertical profile of the partitioning between various families of NSPs containing or not
181 carbonaceous material and metals (Murphy et al., 1998; Jost et al., 2004; Murphy et al.,
182 2007; Murphy et al., 2014). However, from this technique it is difficult to conclude whether
183 the metallic elements are dissolved or are in the form of refractory inclusions in the sulfate
184 particles.

185

186

187

188



189 **2.4 Balloon-borne measurements**

190

191 Stratospheric (zero pressure) balloons can reach 40 km altitude and stay up to a few
192 tens of hours in flight. They are well-adapted to study the middle stratosphere above
193 altitudes reached by airplanes. Measurements can be conducted during ascent, at float and
194 during a slow descent. However, technical and operational constraints strongly restrain the
195 number of flights and the geographic zones for launches.

196 Remote sensing measurements, using natural light sources (Sun, Moon, stars) can
197 provide the vertical profile of aerosols extinction with a resolution of a few hundreds of
198 meters, generally in the UV-visible domain (Renard et al., 2002). For liquid aerosols, the size
199 distribution can be retrieved using Mie scattering calculations. Such an observational
200 method needs to assume that the stratosphere is composed of horizontally homogeneous
201 layers along lines of sight of tens to hundreds of km long, although significant local
202 concentration variations can bias the retrieval (Berthet et al. 2007). Nevertheless, non-
203 monotonous UV-visible extinctions could be an indicator of the possible presence of
204 optically absorbing material in the stratosphere together with the sulfate aerosol population
205 (Berthet et al., 2002; Renard et al., 2002). Also, the measurements of the local radiance
206 scattering function for the aerosols (Mishchenko, et al., 2004) can be used to distinguish
207 between sulfate and other types of particles (Renard et al. 2008). However, such studies
208 have not addressed the possibility for the aerosols to be internally or externally-mixed.

209 The optical aerosol counters are easier to use from balloons than from airplanes,
210 since the relative speed between the instrument and the ambient air is low, around 5m/s
211 during ascent or slow descent and close to zero at float. They can typically detect particles
212 with sizes from about 0.2 μm to a few μm (Deshler et al., 2006; Renard et al., 2005), and
213 provide the vertical profiles of the aerosols for several size classes. An improved optical
214 particle counter has been used to detect the fraction of aerosols that are charged, probably
215 by the galactic cosmic rays (Renard et al., 2013). Such charged particles could have some
216 implication in the high-energy phenomena in the middle and upper atmosphere (Füllekrug et
217 al., 2013).

218 Finally, the negligible speed between the balloon and the ambient air at float altitude
219 is optimal to collect the particles without breaking them. As for airplane collection, the
220 particles are analyzed in the laboratory after a soft landing of the gondola (Testa et al., 1990;
221 Ciucci et al., 2008; Della Corte et al., 2013).

222

223

224 **2.5 Satellite measurements**

225

226 Satellite instruments can provide a global coverage of the aerosol content in the
227 stratosphere (Bingen et al., 2004; Vanhellefont et al., 2010; Vernier et al., 2011; Salazar et
228 al., 2013; Thomason et al., 2018). They can be used to derive trends over several years or to
229 study locally strong sources of aerosols. For such remote sensing measurements, inversion
230 methods are necessary to retrieve the vertical profiles, using assumptions on the complex
231 refractive index of the particles and/or on the shape of the size distribution (e.g. Bourassa et
232 al., 2012). Nevertheless, they cannot access to the local variability of the aerosol content,
233 which can be potentially diluted along the line of sight and/or could be removed when
234 applying smoothing or filtering procedures.



235 The UV-visible extinction measurements obtained from occultation or from limb
236 profiling rely on the hypothesis of homogeneous layers in the stratosphere. The vertical
237 resolution is between one and a few km. Nevertheless, it is possible to follow intense events
238 of injection of refractory material in the stratosphere from fires (carbonaceous particles),
239 volcanoes (ash) and meteoroid disintegration (Fromm and Servranckx, 2003; Fromm et al.
240 2006; Niemeier et al., 2009; Gorkavyi et al., 2013; Rieger et al., 2014). Also, extinction
241 measurements can be used to search for the presence of NSPs with respect to the pure
242 sulfate population in the middle stratosphere (Neely et al., 2011).

243 The space-borne lidar measurements, like the CALIOP instrument onboard the
244 Calipso satellite, are mainly dedicated to cloud studies, tropospheric aerosols and the
245 boundary layer (e. g. Bourgeois et al., 2018), since the scattered signal is often too low for
246 the detection of stratospheric aerosols. Also, reference altitudes used to derive the Rayleigh
247 signature in the lidar retrieval and assumed to be aerosol-free are often too low to detect
248 stratospheric aerosols in general above 30 km altitude (Vernier et al., 2009). Nevertheless,
249 analyses can be conducted during specific events such as a volcanic eruption and injections
250 of carbonaceous particles and/or the gaseous precursors by the Asian monsoon or pyro-
251 convection (Vernier et al., 2016; Govardhan et al., 2017; Vernier et al., 2018; Khaykin et al.,
252 2018).

253 Finally, attempts to collect dust from space entering the Earth's atmosphere were
254 made from Gemini 10, Skylab, Salyut 7 and MIR space stations, and from the retrieval of
255 space exposed surfaces of satellites. The Long Duration Exposure Facility (LDEF) was exposed
256 for almost 6 years at altitudes ranging from 580 km to 332 km, and provided evidence for
257 micrometeoroids (Mandeville et al., 1991; Love and Brownlee, 1993; Kalashnikova et al.,
258 2000) that do enter the Earth's atmosphere.

259
260

261 **3. Regular flights with balloon-borne aerosols counters**

262

263 **3.1 Instruments for stratospheric studies**

264

265 The previous measurements have shown that the stratospheric content of NSPs
266 exhibits a strong horizontal, vertical and temporal variability, since the sources of NSPs can
267 be diverse. Regular and frequent in situ measurements are of high relevance to derive the
268 stratospheric aerosols content and to follow its evolution, because the use of a priori
269 hypothesis on the shape, the composition and the size distribution of the particles
270 commonly used in data retrievals from remote sensing instruments (e.g. Bourassa et al.,
271 2012) is at least minimized or at best pointless. Such measurements strategy with aerosols
272 counters under balloons started about 50 years ago.

273 The University of Wyoming aerosols counters (Deshler et al., 2003; Deshler et al.,
274 2006) and the Stratospheric and Tropospheric Aerosols Counter (STAC) (Renard et al., 2008;
275 Renard et al., 2010) have provided locally the size distribution and the concentrations of
276 aerosols up to 40 km in altitude when launched under (large) stratospheric balloons. In
277 particular, during its 21 flights in the 2004 - 2011 period, STAC has often detected strong
278 aerosol concentration enhancements over a vertical extent from few hundreds of meters to
279 few km.

280 Such instruments were calibrated for the detection of liquid particles typically in the
281 0.2 – 5 μm size range. Since their measurement technique is sensitive to the complex



282 refractive index of the particles, these instruments cannot be used to distinguish between
283 transparent liquid particles and optically absorbing NSPs, the size of the latest being possibly
284 underestimated. The weight of the instrument is of several kg, preventing them to be used
285 under small balloons as weather balloons.

286 Given that the aerosol variability does not necessarily vary homogeneously
287 throughout the stratosphere especially under the influence of sporadic events (volcanic
288 eruptions, fires, meteoroid disintegrations), regular and frequent in-situ measurements must
289 be conducted from several locations in the world. Accounting for operational constraints and
290 cost issues, it seems that the most valuable method is to launch light and inexpensive
291 instruments under weather balloons, sending the data by a telemetry system, with the risk
292 of losing the instrument after the flight. Such types of balloons can reach an altitude of 35
293 km, but the burst of the balloon cannot be controlled. The payload weight must be below a
294 few kg to account for the international aeronautic rules. The cost for the balloons and the
295 gas are no more than a few hundreds of euros. Two or three people are necessary to launch
296 the balloon from almost everywhere in the world. The wind speed at ground could be up to
297 15 m/s. Then, frequent measurements, typically tens of flights per year, can be conducted
298 regularly and during specific events almost from everywhere.

299 Light instruments are not currently available for collecting systems or for mass-
300 spectrometry. On the opposite, two light optical aerosols counter with a weight of about 1
301 kg are now available on the market. The first one is the Printed Optical Particle Spectrometer
302 (POPS), designed for the detection of liquid particles in the $\sim 0.15 - 1 \mu\text{m}$ size range (Gao et
303 al., 2016). It can provide very accurate size distributions and concentrations of sub-micronic
304 sulfate stratospheric aerosols with a vertical resolution of 100 m or better, but is not
305 designed to detect the largest particles previously detected in the stratosphere (e.g.
306 Jessberger et al., 2001; Ciucci et al., 2008) and cannot identify the optically absorbing
307 particles. The second one is the Light Optical Aerosols Counter (LOAC). LOAC is a novel
308 instrumental concept (Renard et al., 2016a), providing the size distributions, the
309 concentrations, and an estimate of the typology, for particles in the 0.2 - 50 μm size range.
310 LOAC uses a statistical approach to retrieve the concentration of particles smaller than 1 μm
311 (Renard et al., 2016a). When the concentration of submicronic particles is low, typically
312 below 10 particles cm^{-3} for sizes greater than 0.2 μm , the integration time must be increased
313 up to 10 min; then the vertical resolution is between 1 km and 3 km for a balloon ascent
314 speed of about 5 m/s. Since LOAC is not sensitive to the complex refractive index of the
315 particles, it can detect all particle types. LOAC is well appropriated for the detection of the
316 NSPs, as previously shown for dust particles in the troposphere (Renard et al., 2018), while
317 the POPS is better designed for the detection of the submicronic sulfate aerosols; then these
318 two instruments could be considered as complementary.

319
320

321 **3.2 The LOAC instrument**

322

323 The particles are injected through an optical chamber by a pumping system, cross a
324 laser beam and the light scattered by the particles is recorded by two detectors.
325 Conventional aerosols counters typically performed measurements at large scattering angles
326 (greater than 30° and often around 90°). Since the scattered light is sensitive to the size of
327 the particles but also to their complex refractive index and their shape including porosity
328 effects, conventional optical counter measurements must be corrected for the nature of the



329 particles. On the opposite, LOAC performs measurement at small scattering angles, in the
330 11°-16° range, where the scattered light is mainly coming from diffraction that does not
331 depend on the complex refractive index nor on the porosity of the irregular-shaped particles
332 (Lurton et al. 2014). As a result, a direct correspondence between the intensity of the
333 scattered light and the optical diameter of the particles becomes feasible. LOAC provides
334 particles number concentrations for 19 sizes in the 0.2 – 50 μm size range, with an
335 uncertainty of $\pm 20\%$ for concentrations higher than 10 particles cm^{-3} ; the uncertainty
336 increases to about $\pm 30\%$ for submicronic particle concentrations higher than 1 particle cm^{-3} ,
337 and to about $\pm 60\%$ for concentrations smaller than 10^{-2} particle cm^{-3} . The size of the
338 particles provided by LOAC is an optical diameter, which could differ from aerodynamical,
339 electric mobility and gyration diameters used by other counting techniques in case of
340 irregular particles. Also, the refractory particles could be hydrated, thus having a size greater
341 than dry particles. The ability of LOAC to accurately detect micron-sized particles and larger
342 particles has been validated during numerous intercomparison sessions with different
343 instruments (Renard et al., 2016a; Renard et al., 2018).

344 LOAC has a second detector at a scattering angle in the 50°-70° range, where the
345 scattered light is very sensitive to the complex refractive index and to the porosity of the
346 particles. By statistically combining these measurements with those at 11-16°, we obtain a
347 parameter called “speciation index”, which is representative of the properties of the
348 particles to absorb light (Renard et al., 2016a). Higher is the speciation index, darker are the
349 particles. Speciation index reference measurements were conducted in laboratory with pure
350 reference samples to establish a data base. By comparing the ambient air measurements to
351 the database, we can tentatively identify the basic nature of the particles, or typology. As
352 confirmed during tests in laboratory and in ambient air, LOAC can indicate if the detected
353 aerosols are icy, are in a non-optically absorbing liquid phase as the typical stratospheric
354 pure sulfate population, are semi-transparent NSPs as some dry minerals or highly hydrated
355 solid aerosols, or are optically-absorbing NSPs as carbonaceous particles. For the last case, it
356 is not possible however to know if the particles are externally or internally-mixed with
357 sulfate, or can be considered as a secondary organic aerosol. This approach is just a first step
358 to validate the ability of optical measurements to provide an estimate of the nature of the
359 stratospheric aerosols.

360 The raw LOAC concentrations are corrected of the sampling efficiency when the
361 measurements are conducted under weather balloon (Renard et al., 2016a), the sampling
362 being dominated by sub-isokinetic conditions and the divergence of the flow field at the inlet
363 entrance.

364
365

366 **3.3 Vertical profile of aerosol concentrations obtained with LOAC**

367

368 The LOAC gondola includes batteries, telemetry to send the data in real time, and
369 temperature and humidity sensors, using the MeteoModem Company system (Renard et al.,
370 2016b). Since May 2013 to mid-2019, 135 flights reaching the stratosphere have been
371 successfully conducted from France, from Spain and from Ile de la Réunion (Indian Ocean).
372 Regular flights, from one to four per month, have been operated since February 2014 from
373 France mainly by Centre National d’Etudes Spatiales (CNES), the French Space Agency, from
374 its balloons launching base at Aire sur l’Adour (43.70°N, 0.25°W); in this case the balloons
375 are called “Light Dilatable Balloons” since they carry a scientific instrument, to distinguish



376 them for conventional weather balloons. Figure 1 presents a LOAC launch from Aire sur
377 l'Adour on 6 February 2014.

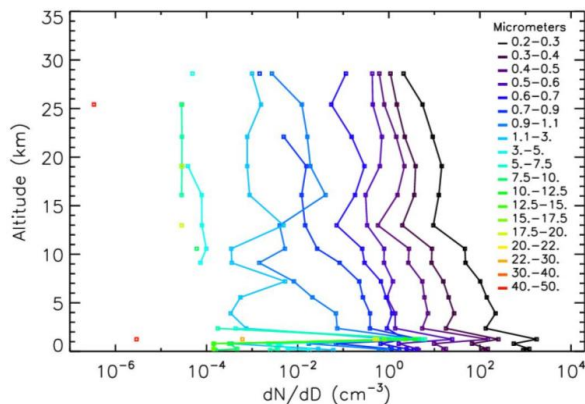
378 Figure 2 presents an example of the vertical evolution of the particle number
379 concentrations for a LOAC flight in 17 August 2017, again from Aire sur l'Adour.
380 Concentrations decrease with altitude, as expected for sulfate aerosols. The retrieved
381 typologies in the stratosphere indicate that the submicron aerosols are indeed transparent
382 liquid droplets based on the comparison with reference curves obtained in the laboratory
383 with this type of particles (Figure 3). Note that in this example the number of detected
384 particles for size classes above $3\ \mu\text{m}$ is too low for the typology determination.

385 Few particles greater than $5\ \mu\text{m}$ are detected above the tropopause, and one particle
386 larger than $40\ \mu\text{m}$ is present at 25 km altitude. Since the flight was conducted while the
387 permanent Perseids meteor shower took place, one could suggest that LOAC has detected
388 some dust particles coming from space.
389



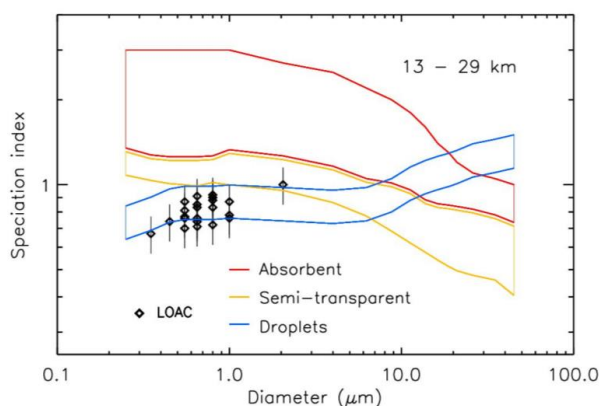
390
391
392

Figure 1: LOAC launch from Aire sur l'Adour (France; 43.70°N , 0.25°W) on 6 February 2014



393
394
395
396
397

Figure 2: Vertical profile for the LOAC 17 August 2017 flight from Aire sur l'Adour (France; 43.70°N , 0.25°W) during the Perseids meteor shower period. Errors bars (see text) are omitted for clarity reasons



398

399

Figure 3: Indications of typology from the LOAC speciation index in the stratosphere for the 17 August 2017 flight

400

401

402

403

LOAC has detected some strong vertical variability of aerosol concentrations during flights in background conditions (without recent volcanic eruptions). We consider here that a strong concentration enhancement is detected whenever the concentrations are at least 5 times higher than the background concentrations measured during the same flight for at least 5 consecutive size classes (this criterion is to ensure that the enhancements are real and are not due to noise measurement fluctuations). We exclude the measurements conducted at the edge of the polar vortex where the local dynamical variability can affect the aerosols content (Renard et al., 2008).

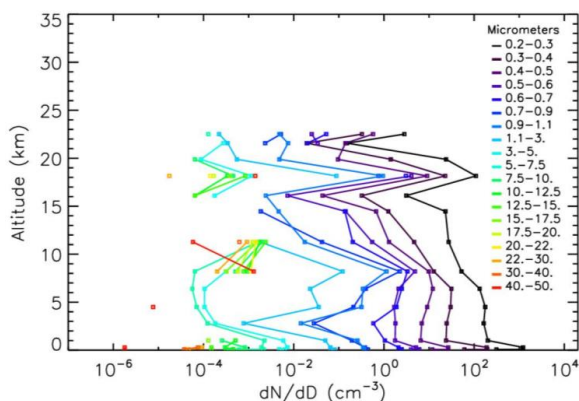
411

Figure 4 presents an example of a strong concentration enhancement in the lower stratosphere at an altitude of 18 km, as observed during a flight conducted from Aire sur l'Adour on 11 August 2016, during the Perseids period. Several particles bigger than 5 μm have been also detected at this altitude, which could result from the fragmentation of a larger fluffy particle or could be an accumulation layer of carbonaceous particles (note that the large particles between 8 and 12 km altitude correspond to a cirrus cloud). The typology (Figure 5) indicates that particles up to 2 μm are indeed in liquid phase, in this case certainly sulfates, while biggest ones are classified as strongly optically-absorbing NSPs.

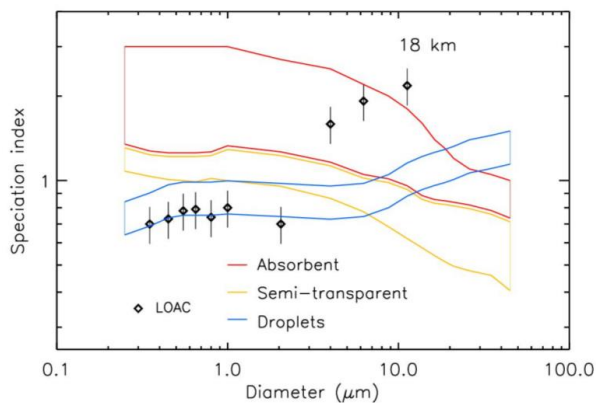
419

Figure 6 presents another example of concentration enhancement observed in the middle stratosphere at an altitude of 28 km and only for submicronic particles, during a flight on 23 November 2017 from Aire sur l'Adour. This time, the typology (Figure 7) indicates mainly optically-absorbing particles for the smaller size classes.

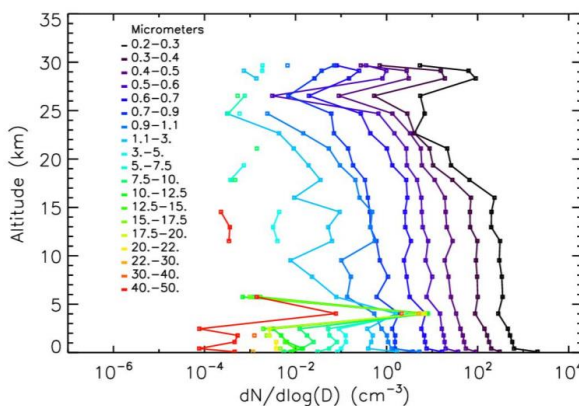
423



424
425 *Figure 4: Vertical profile for the LOAC 11 August 2016 flight from Aire sur l'Adour (France;*
426 *43.70°N, 0.25°W) during the Perseids meteor shower period. Errors bars (see text) are*
427 *omitted for clarity reasons*
428



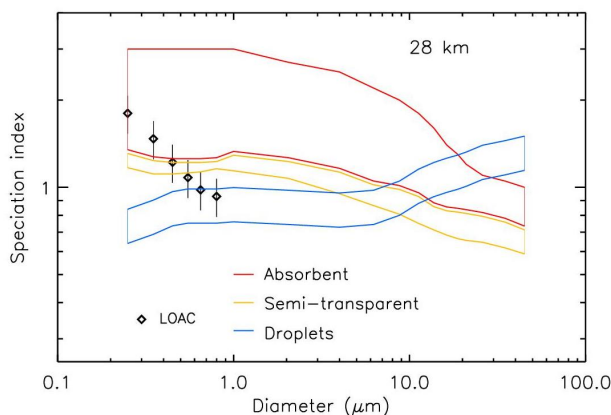
429
430 *Figure 5: Indications of typologies from the LOAC speciation index in the stratosphere for the*
431 *11 August 2016 flight*
432



433
434 *Figure 6: Vertical profile for the LOAC 23 November 2017 flight from Aire sur l'Adour (France;*
435 *43.70°N, 0.25°W). Errors bars (see text) are omitted for clarity reasons*



436



437

438

Figure 7: Indications of typologies from the LOAC speciation index in the stratosphere for the 23 November 2017 flight

439

440

441

442

443

444

445

446

447

448

449

450

451

452

453

454

455

456

457

458

459

460

461

462

463

464

465

466

467

468

469

As a result, within the error bars, we can conclude that LOAC seems to have detected similar concentration enhancements as those previously reported from STAC measurements, although the two instruments use different geometries of observation. About 25% of the 135 LOAC and 21 STAC flights exhibit such strong enhancements. The enhancements could be sometimes only for submicronic particles, and sometimes for all size classes up to more than 10 μm . The typology measurements indicate that most of the enhancements are dominated by NSPs particles: nevertheless, the speciation index varies from one flight to another from semi-transparent to strongly absorbent particles, which could indicate that several families of NSPs were detected. To attribute the origin of these detections, it is necessary to review the already published results on NSPs detections obtained by the various instrumental techniques.

4. Previous studies on the spatial and temporal variability, size and composition of NSPs

4.1 Vertical dependence of NSP particles

In the middle and upper stratosphere, Neely et al. (2011) have compared the SAGE II satellite extinctions to model calculation (WACCM) assuming only liquid aerosols. They have found strong enhancement of measured extinction above 30 km altitude on average; a mean extinction value of about $5 \cdot 10^{-6} \text{ km}^{-1}$ is found at 40 km altitude although model calculations provide a zero value for sulfate aerosols. The extinction enhancements are associated with the contribution of meteoritic smoke particles, coming from the disintegration of meteorites or micrometeorites and recondensation processes (Plane, 2003; Plane et al., 2018; Rapp et al., 2007; Bardeen et al., 2008; Plane, 2012), while an external and/or internal mixture of smoke particles and sulfate aerosols occur at lower altitudes. The ubiquitous presence of non-optically transparent particles was also found in the extinction measurement by



470 GOMOS/Envisat, at the same altitudes as SAGE II, for which the wavelength dependence of
471 the extinction strongly differed from the one expected for liquid aerosols only (Salazar et al.,
472 2013). The presence of light-absorbing particles in the middle stratosphere was also
473 detected from sparse balloon measurements with extinctions and radiance measurements
474 (Renard et al., 2005; Renard et al., 2008); these particles could be either internally or
475 externally-mixed with the sulfate aerosols. Nevertheless, such remote sensing
476 measurements do not provide the precise nature and composition of these particles, so-
477 called “soot” by the authors although “strongly optically-absorbing material” could be more
478 appropriate (the terminology for describing such light-absorbing carbons is reviewed in Bond
479 and Bergstrom (2007)).

480 The presence of soot and BC in the lower stratosphere was detected below 20 km
481 altitude using wire impactors on airplane (Pueschel et al., 1992; Blake and Kato, 1995;
482 Strawa et al., 1999). According to Strawa et al. (1999), BC aerosol number density could be
483 of about 1 % of the total aerosols content in the lower stratosphere. On the other hand,
484 Baumgardner et al. (2004) have studied the concentration of light-absorbing particles
485 (attributed to BC and particles with metals) in the 0.2-0.8 μm size range above the
486 tropopause in the northern polar vortex by light scattering and incandescence
487 measurements, and found more than 10 particles cm^{-3} in that size range. These light
488 absorbing particles are more concentrated by a factor of 10 than the non-light absorbing
489 particles below 0.3 μm inside the polar vortex, with higher contents than for extra-vortex air.
490 Similarly, by using counting techniques and heating to remove the volatile material, Curtius
491 et al. (2005) found a much higher fraction of particles containing non-volatile residues inside
492 than outside the polar vortex. These particles could result from the downward transport of
493 refractory meteoritic material within the polar vortex from the mesosphere to the lower
494 stratosphere as concluded from aerosol collections (Weigel et al., 2014; Ebert et al., 2016).

495 At other latitudes, Murphy et al. (2007, 2014) have derived two categories of NSPs
496 for altitudes below 20 km at different latitudes, using Particle Analysis by Laser Mass
497 Spectrometry (PALMS) observations: NSP with metal compounds proposed to probably
498 originate from vaporized and condensed meteoritic material, and NSP with mixture of
499 sulfate and organic particles. The second category corresponds to the main components of
500 aerosols in the mid-latitude and tropical lower stratosphere. These observations agree with
501 the Schwarz et al. (2006) results in the northern tropical region, where 40% of BC particles
502 showed evidence of internal mixing. Then, the average fraction of carbonaceous material in
503 the stratospheric particles decreases rapidly with increasing altitude.

504

505

506 **4.2 Sporadic strong enhancements in the stratospheric aerosol content from NSPs**

507

508 Several authors have reported local enhancements of NSP concentrations in the
509 stratosphere. These sporadic features are highly variable in term of residence times (i.e.
510 from the scale of days to months).

511 Jost et al. (2004) have detected plumes of carbonaceous particles originating from
512 North American forest burning in July 2002 up to an altitude of 16 km by Laser Mass
513 spectrometry and counting measurement. The increase concentration is about 7 times
514 higher than background conditions. The origin of the particles was confirmed with correlated
515 CO measurements. Short-living and local increases up to a factor 2.5 in aerosol extinction
516 measurements related to intense biomass burning have been seen by the SAGE III space-



517 borne instrument over Australia at the beginning of 2003 (Fromm et al. 2006). These
518 particles can be injected in the lower stratosphere by the pyroconvection process occurring
519 at the top of the dense smoke clouds (Fromm and Servranckx, 2003). Ground-based lidar
520 measurements at Observatoire de Haute Provence, France (43.9°N, 5.7°E) and space-borne
521 lidar measurements from the CALIOP/Calipso instrument have detected plumes of fire
522 particles between 18 and 20 km altitude over southern France, coming from wildfires in
523 northwest Canada and United States in August 2017 (Khaykin et al., 2018). The scattering
524 ratio at 532 nm wavelength is about 10 times higher than for background conditions. Also, a
525 layer of soot particles at 15-16 km altitude coming from these wildfires, and well identified
526 by the specific wavelength dependence of the lidar depolarization ratios, were observed in
527 Germany over Leipzig (51.3°N, 12.4°) on 22 August 2017 (Haarig et al., 2018). These
528 measurements have shown that local enhancements of fire plume particles can be detected
529 several thousands of km from their sources, impacting the stratospheric aerosol content at
530 the hemispheric scale, with an amplitude (both in terms of aerosol content and residence
531 time) comparable to that of a moderate volcanic eruption (Peterson et al., 2018). Satellite
532 data show that the NSPs from this specific fire plume event remained detectable in the
533 northern hemisphere stratosphere over a period of about 8 months (Kloss et al., 2019).
534 Nevertheless, the morphology and composition of these particles have not been determined
535 so far.

536 Local intrusions of particles attributed to BC have also been reported from
537 CALIOP/Calipso in the lower stratosphere during the monsoon season over India, with few
538 sparse enhancements by 20-30 km altitude (Govardhan et al., 2017). The origin of such
539 particles is not well-established though these authors propose them to originate from
540 airplanes traffic before being vertically transported.

541 Moderate volcanic eruptions can inject aerosols directly into the lower stratosphere.
542 Some ashes can be present, as observed after the Kelud eruption (February 2014) in the
543 lower tropical stratosphere (Vernier et al., 2016). Ashes were detected by analysis of
544 CALIOP/Calipso space-borne observation in comparison with in situ measurements from
545 optical backscatter aerosols sounders and optical aerosols counters. The residence time of
546 ash material in the stratosphere depends on the injection altitude and on the size of the
547 particles. Values of several weeks are expected due to sedimentation (Niemeier et al., 2009).
548 However, the residence time of ash material is not clearly determined especially when
549 mixing or coating processes with sulfate occur.

550 Rockets produce solid particles that can be found in the stratosphere. Campaigns of
551 in-situ particle counter measurements were conducted on board airplanes in 1996 and 1997
552 to detect the alumina particles in the motor exhaust plumes. Measurements in the
553 stratosphere between 17 and 19.5 km showed strong concentration enhancements of about
554 a factor of 100 with respect to the nearby background conditions (Ross et al., 1999).

555 The ground-based twilight photometric observations have shown accumulation
556 layers at altitudes of 30 km and 54 km on 20-21 November 1998 during the Leonids meteor
557 shower (Mateshvili et al., 1999). Large and thin dust accumulation layers were also detected
558 between 20 and 50 km altitude on 21-26 November 2001, 25-27 November 2002, and 16-17
559 November 2003 during the Leonids (Padma Kumari et al., 2005). The Leonids, as opposed to
560 permanent meteor showers visible on every year at a given epoch, may produce periodic
561 meteor storms, for about 3 to 4 years, every 33 years, in November. The enhancements in
562 the twilight light intensities are of tens of percent. Such layers were observed 4 to 8 days
563 after the peak meteor activity, but with a strong variability from one day to another for the



564 altitude and the amplitude of the vertical structures. The authors state that, a couple of
565 weeks after the meteor activity, the atmosphere had recovered its normal dust distribution
566 profile although a dust layer at 30 km altitude could have persisted. Such observations of
567 transient layers need to be confirmed for other occasional and major meteor storms.

568 Some lidar observations in the Arctic during the 2000-2001 winter have fortuitously
569 detected strong concentration enhancements from 25 to 40 km altitude, with strong spatial
570 and temporal variability over a few days (Gerding et al., 2003). It has been proposed that
571 they could originate from meteoritic debris after the disintegration of a meteoroid in the
572 atmosphere or from debris of condensed rocket fuel. Klekociuk et al. (2005) have also
573 observed a strong particle enhancement around 30 km altitude, which was well identified as
574 coming from the disintegration of a large meteoroid of a few meters in size on 3 September
575 2004 over Antarctica, with residence time from weeks to months.

576 Major meteoritic disintegrations can produce strong enhancements in aerosol
577 concentrations, initially localized at the altitude of the disintegration and then progressively
578 dispersed by the global circulation. The Chelyabinsk meteor event on 15 February 2013
579 started with an enhanced aerosol loading in the 30-35 km altitude range, as seen in
580 extinction measurements of the OSIRIS/ODIN satellite instrument (Rieger et al., 2014). OMPS
581 instrument onboard the Suomi NPP spacecraft has detected an extinction enhancement of a
582 factor 10 at 40 km altitude and a few km width. It has also monitored the motion of the
583 associated ring-shaped plume in the mid-latitude stratosphere, over at least 3 months,
584 through its dispersion and its sedimentation from 40 to 30 km altitude (Gorkavyi et al.,
585 2013).

586 Such local concentration enhancements in the middle stratosphere, at least 5 to 100
587 times higher than background levels, have been occasionally detected by the balloon-borne
588 Stratospheric and Tropospheric Aerosols Counter (STAC) having operated from 2003 to 2011
589 (21 flights) at various latitudes (Renard et al., 2008; Renard et al., 2010). Such enhancements
590 were mostly detected in the middle stratosphere. Although the instrument has not been
591 designed to distinguish between liquid and optically-absorbing particles in terms of sizing,
592 particles up to 5 μm were detected in some enhancements, unlikely to be pure sulfuric acid
593 aerosols at such altitudes. In particular, 8 STAC flights were conducted above northern
594 Sweden from 2 August to 7 September 2009, showing a strong variability from one day to
595 another of the aerosol content and transient enhancements in the middle stratosphere
596 (Renard et al., 2010). The enhancements could be very local, i.e. of a few km in term of
597 horizontal extent (Renard et al. 2008).

598
599

600 **4.3 Size distribution**

601

602 The size distributions of NSPs in the stratosphere are poorly estimated. Indications
603 have been mainly obtained by optical counters and by in-situ collectors with analyses by
604 electron microscopy at ground.

605 Hunten et al. (1980), combining modeling calculations of the meteorite ablation
606 around 80 km altitude and airplane collected particles (Brownlee, 1978), has proposed a
607 bimodal repartition of the solid material in the middle stratosphere. The particles below 0.1
608 μm could come from the descending smoke particles, while the largest particles could
609 originate from interplanetary dust and meteoritic debris. Nevertheless, the real content of
610 NSPs could be more complex.



611 In the lower stratosphere, different size distributions have been detected. In the
612 Arctic, the optically-absorbing particles can dominate for size below $0.3\ \mu\text{m}$ (Baumgardner et
613 al., 2004). The rocket engine plumes measurements, for the two cases-studies in the 17-19.5
614 km altitude range, have shown a three modal distribution centered below $0.01\ \mu\text{m}$, around
615 $0.1\ \mu\text{m}$ and around $2\ \mu\text{m}$ (Ross et al., 1999). The fine volcanic ashes in the lower tropical
616 stratosphere after the Kelud eruption have been estimated to be below $0.6\ \mu\text{m}$ in optical
617 diameter (Vernier et al., 2016). The PALMS instrument, which has detected two families of
618 NSPs in the lower stratosphere, has shown that the particles have an aerodynamical
619 diameter below $1\ \mu\text{m}$ (Murphy et al. 2014). However, the instrument works only in the 0.2-2
620 μm size range and the aerodynamical diameter can significantly differ from the optical
621 diameter used by the optical aerosol counters.

622 The particles collected from airplanes present a wide variety of shapes and sizes. Soot
623 particles are in general smaller than $1\ \mu\text{m}$, in a compact or chain-like shapes (Pueschel et al.,
624 1992; Blake and Kato, 1995; Strawa et al., 1999). Submicronic to $10\text{-}\mu\text{m}$ particles of very
625 different shapes and natures were collected by Ebert et al. (2016) in the stratospheric polar
626 vortex at altitudes up to 21 km (Figure 8). Large particles, from a few μm to a few tens of
627 μm , are also present in the NASA aircraft JSC dust collections (Jessberger et al., 2001;
628 Sandford et al., 2016) and in the balloon-borne dust collection by the DUSTER instrument
629 (Ciucci et al., 2008). The concentrations of particles greater than a few μm could be in the
630 $10^{-6}\text{-}10^{-3}$ particles cm^{-3} range.

631
632

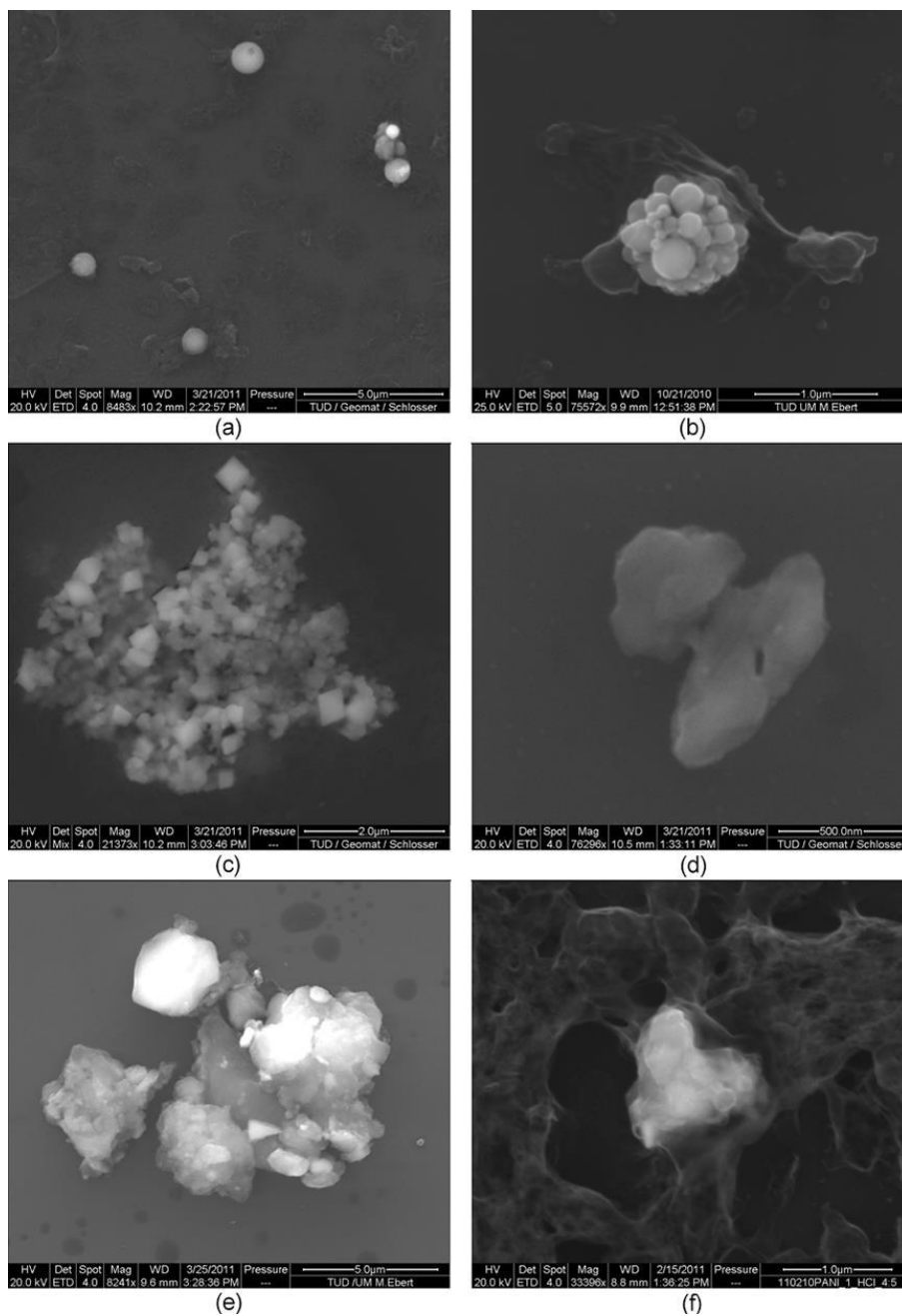
633 4.4 Particles chemical composition

634

635 In the lower stratosphere, the presence of an aerosol population with mixed sulfuric
636 acid and metals, principally Fe, Na, K, Al, Cr, Ni atoms, has been derived from airborne mass-
637 spectrometry observations (Murphy et al., 1998; 2014). Soot or BC particles have been also
638 detected, in agreement with other observations (Blake and Kato, 1995; Strawa et al., 1999).
639 Also, Scott and Chittenden (1993) have shown from collected particles that the composition
640 of particles below $0.2\ \mu\text{m}$ strongly differs from that of the common pure sulfate aerosols;
641 the main population of these ultrafine particles is composed of carbon, with traces of S, Na,
642 metal sulfates and chlorides.

643 The analysis of hundreds of airplane-collected NSPs in the polar winter lower
644 stratosphere by Ebert et al. (2016) has shown that refractory particles greater than $0.5\ \mu\text{m}$
645 mostly consist of silicate, silicate/carbon mixtures, Fe-rich, Ca-rich, and complex metal
646 mixtures including aluminum. The detection of metallic spheres within some mixed particles
647 might indicate the effect of high temperatures during the formation process but is not in line
648 with the results from airborne mass spectrometers which might rather suggest diluted Fe
649 atoms (Murphy et al., 2014). On the other hand, particles below $0.5\ \mu\text{m}$ are mostly
650 composed of soot (Ebert et al., 2016). Most of these submicronic carbonaceous refractory
651 particles are completely amorphous and only a few particles are ordered with graphene
652 sheets (Schütze et al., 2017); minor traces of Si, Fe, Cr, Ni are often found in these
653 carbonaceous particles, and no difference has been highlighted in terms of size,
654 nanostructure and elemental composition for such particles either collected inside and
655 outside the polar vortex at least for the period of these observations, i.e. winter 2010.

656



657
658 *Figure 8: Examples of particles collected from an airplane (Figure 3 of Ebert et al. 2016),*
659 *showing their diversity in size, morphology and composition. The electron-microscope images*
660 *present refractory particles of (a) silicate spheres, (b) Fe-rich particle; (c) complex metallic*
661 *mixture (Al / Cr / Mn / Fe), (d) Ca-rich particle, (e) carbon /silicate mixture, and (f) silicate*
662 *particle*
663



664

665 Amongst the huge number of particles collected by the NASA airplane in the lower
666 stratosphere, particles assumed to be chondritic porous interplanetary dust, also named CP
667 IDPs, are composed of optically black aggregates of submicron components, with a wide
668 range of porosities (Rietmeijer, 1998). They are significantly enriched in carbon, most likely
669 in the form of pristine and complex organic molecules (Thomas et al., 1993; Flynn et al.,
670 2013; Koschny et al. 2019). Similarities between these particles and cometary dust particles
671 have been progressively suggested by analyses of samples from the Stardust flyby mission at
672 comet 81P/Wild 2 (Ishii et al., 2008), and more recently established through results on the
673 composition and the physical properties of cometary dust from the long-duration Rosetta
674 mission with comet 67P/Churyumov-Gerasimenko (Levasseur-Regourd et al., 2018; Mannel
675 et al. 2019). Also, the carbonaceous micrometeorites collected in Antarctica, also named
676 UCAMMs for Ultra Carbonaceous Antarctica Micro-Meteorites (Engrand and Maurette,
677 1998), after partial survival to the atmospheric entry and thus short transit in the
678 stratosphere, are estimated to be of cometary origin with up to 85% of organic matter in
679 volume (Nakamura et al., 2005; Dartois et al., 2018; Levasseur-Regourd et al., 2018) mixed
680 with tiny flakes of minerals.

681 In the middle stratosphere, Testa et al. (1990) have found Cl, S, Ti, Fe, Br, Ni, Zr, Zn,
682 Sr, and Cu elements to be present in the aerosols (elements having atomic number lower
683 than 16 could not be detected in their analysis), with 2/3 of the 23 analyzed non-graphitic
684 particles ranging from Al rich silicates to almost pure Fe, and one particle consisting-almost
685 exclusively of Ba and S. The DUSTER collection has shown also two 100 μm spheres with O-
686 Si-Na-Mg-Ca composition (Ciucci et al., 2008) and the presence of pure carbon particles,
687 aggregates of CaCO and CaCO₃ grains (Della Corte et al., 2013).

688

689

690 **5. Sources from ground to space**

691

692 **5.1 Context**

693

694 All the information derived from the previously described reported studies appears
695 difficult to reconcile in terms of NSP concentrations, size distributions, and compositions. In
696 fact, most of the measurements could represent snapshots on specific geophysical
697 conditions. The strong vertical, temporal and typology variabilities of NSPs detected by LOAC
698 from one flight to another over a 6-year period seem to confirm the complexity of the
699 stratospheric NSP content and the difficulty to propose a global view of particles' origins.

700 Multiple sporadic and permanent sources of NSPs must be considered, coming from
701 Earth (emitted from the surface or produced within the atmosphere) and from space. In
702 particular, some authors have mentioned (disintegrated) meteoritic material, which is
703 indeed a source, but did not always consider porous carbonaceous interplanetary dust
704 particles as mainly originating from comets on prograde orbits. The grains resulting from
705 meteoritic disintegration could differ in size, shape and composition of those coming from
706 the interplanetary dust cloud. The recent results of the Rosetta mission on comet
707 67P/Churyumov-Gerasimenko have provided a ground-truth for such particles.

708 We present below the different sources of the NSPs from ground to space that can be
709 found within the stratosphere. The table 1 summarizes the main characterizes of such
710 particles.



711

Nature	Typical size	Source	Origin
Volcanic ashes	< 0.6 μm	From ground	Natural
Biomass burning	< 1 μm	From ground	Natural
Pollution	< 1 μm	From ground	Anthropogenic
Polymeric nanocomposites	> 1 μm	Produced in the atmosphere	Natural
Rocket exhaust plume	< 5 μm	Produced in the atmosphere	Anthropogenic
Airplane soot	< 1 μm	Produced in the atmosphere	Anthropogenic
Meteoritic disintegration	All sizes	From space and produced in the atmosphere	Natural
Satellite disintegration	All sizes	From space and produced in the atmosphere	Anthropogenic
Interplanetary / cometary dust	< 1 m	From space	Natural

Table 1: Summary of the various sources of NSPs

712

713

714

715 5.2 Sources from Earth's surface

716

717 The presence of volcanic ashes in the stratosphere associated with some volcanic
718 eruptions is due to an explosive process injecting directly the material into the stratosphere.
719 No mechanism of injection of ashes in the troposphere with subsequent transport to the
720 stratosphere by the Brewer-Dobson circulation has been reported so far.

721 Major biomass burning and organic fuel burning, having natural or anthropogenic
722 origin, are more frequent and can produce thick clouds of carbonaceous particles that can
723 reach the tropopause level. These particles can reach the lower stratosphere through direct
724 injection by cross-tropopause pyroconvection events or through transport of fire plumes
725 associated with overshooting convective systems (Damoah et al., 2006; Fromm et al., 2005;
726 de Laat et al., 2012). Also, they might be injected directly in the stratosphere through the
727 tropopause folds at tropical latitudes.

728 In addition to these sporadic events, periodic atmospheric mechanisms can consist in
729 a source of NSPs at a global scale. In particular, the Asian summer monsoon and the
730 associated Asian Monsoon Anticyclone (AMA) largely determine the composition of the
731 Upper Troposphere / Lower Stratosphere (UTLS). An accumulation of aerosols has been
732 pointed out inside the AMA and is present each year from June to September in the ~15-18
733 km altitude range in the UTLS region. This layer, known as the Asian Tropopause Aerosol
734 Layer (ATAL) (e.g. Vernier et al., 2018), is likely to be associated with Asian emissions of
735 anthropogenic pollutants like sulfur dioxide and volatile organic compounds, building a
736 population of NSPs consisting of a mixture of sulfates and organic material both as primary
737 and secondary organic aerosols. The ATAL is sustained by the convective activity of the Asian
738 monsoon as indicated by global model simulations (Yu et al., 2015; Fadnavis et al., 2017).
739 However, the precise composition, variability, trend and budget of the ATAL are still largely
740 uncertain and are currently under investigation. After the breakup of the AMA, the signature
741 of the ATAL is detectable on the extratropical aerosol budget in the northern hemisphere



742 (Khaykin et al., 2017) indicating that combined processes, i.e. emissions in Asia, convective
743 activity and general circulation, impact part of the global stratospheric NSP population.

744

745

746 **5.3 Production within the atmosphere**

747

748 If soot particles emitted from airplane engines can be directly injected in the lower
749 stratosphere during their cruise, their contribution is expected to be low with respect to
750 other sources coming from natural and anthropogenic biomass burning (Baumgardner et al.,
751 2004; Hendricks et al., 2004; Schwarz et al., 2006), although the air traffic is increasing.

752 Hypothetical long-lived volcanic soot particles could be also produced in the
753 stratosphere due to thermal decomposition of methane in the volcano eruption column
754 (Zuev et al., 2014, 2015), but this process need further studies and confirmation.

755 The rockets exhaust and the disintegration of satellites subsequently to their entry in
756 the Earth's atmosphere produce locally alumina, hydrocarbon and metallic debris (Ross et
757 al., 1999; Cziczko et al., 2002). The local content of these specific refractory NSPs increases
758 whenever measurements are fortuitously conducted inside a plume (Newman et al., 2001).
759 Such particles can be also collected far from their sources at different times of their transit in
760 the atmosphere during which their physical properties are likely to evolve. As a result, some
761 of them have been found to be mixed with particles having other origins (Ebert et al., 2016).

762 Compact particles and filaments having 5-10 μm in size and up to several mm long,
763 composed of carbon polymeric nanocomposites, can be produced in ambient air inside
764 plasmas (Hamdan et al., 2017). Such conditions occur during atmospheric entries of
765 meteorites and satellites/rocket debris and during storm lightning (Courty and Martinez,
766 2015) and perhaps during high-energy phenomena in the stratosphere such as blue jets and
767 sprites. These nanocomposites are characterized by the presence of Fe-Ni-Cr elements.
768 Some of the grains collected by Ebert et al. (2016) present the same composition and could
769 be nanocomposites produced within the atmosphere instead of meteoritic material. Also,
770 dusty plasma spherical particles typically in the 0.1-1.5 μm size range can be produced in
771 glow discharge (Pereira et al., 2005) as those encountered in the atmosphere. Layers of such
772 particles (spheres and filaments) could produce significant local concentration
773 enhancements of micron(s)-sized aerosols.

774 The rare events of the disintegration of large meteoroids, with sizes above about 10
775 m, occur several times per century and can produce a large plume of dust that can take
776 months to sediment, as for the Chelyabinsk meteor in February 2013. Disintegration of
777 meter-sized meteoroids is detected several times per year and can produce local layers of
778 dust. And partial or total disintegration of cm-size meteoroids could occur daily. The
779 disintegration altitude depends on the velocity entry, the incidence angle of the trajectory,
780 the density and the composition of the meteoroid (minerals like olivine, iron, ices, complex
781 organics; e. g. Fortov et al., 2013; Coulson et al., 2014). The probability of crossing such a
782 layer fortuitously during in-situ measurements is very low but non-negligible.

783 Meteoritic ablation may begin by altitudes of about 180 km. Layers of minerals and
784 metals are then present in thermosphere between 100 and 80 km altitude from the
785 recondensation process (Rapp et al., 2007; Bardeen et al., 2008; Plane, 2012) that produce
786 nanometer-sized smoke particles (Antonsen et al., 2017). Such NSPs need to be aggregated
787 or to grow through the condensation of sulfuric acid when transported downward to
788 produce particles of at least of 150 nm to be optically detectable by optical aerosol counters.



789

790

791 **5.4 Dust from space**

792

793

794

795

796

797

798

799

The Earth orbits around the Sun within the interplanetary dust cloud, which is a wide and flattened circumsolar cloud built of dust particles (e.g. Koschny et al. 2019). Their sizes range from a few tens of nm to a few decimeters, with dominant sizes around hundreds of μm . The spatial density of the interplanetary dust cloud increases towards the Sun and its near-ecliptic symmetry surface, although it remains extremely low, with about 5 to 20 particles of about 10 μm size per km^3 in the vicinity of the Earth (e. g. Levasseur-Regourd et al., 2001).

800

801

802

803

804

805

806

Since particles within such a size range slowly spiral towards the Sun (under Poynting-Robertson effect), the existence of the interplanetary dust cloud indicates that a more or less continuous replenishment takes place. Interpretation of observations in the visible and infrared domains (Lasue et al, 2007; Rowan-Robinson and May, 2013) and dynamical studies (Nesvorný et al., 2010) indicate that most of the interplanetary dust particles reaching the Earth's vicinity are of cometary origin, with a contribution of about 85% of the total mass influx from short-period comets with a prograde motion, called JFCs (Jupiter Family Comets).

807

808

809

810

811

812

Dust particles of cometary origin have long been understood to form meteoroid streams, such as the August Perseids from comet 109P/Swift-Tuttle. Besides, infrared observations have allowed the discovery of faint dust bands, attributed to collisions within the asteroid belt (Dermott et al., 1984) and of narrow and elongated structures (so-called dust trails) along JFCs (Sykes et al. 1986; Reach et al. 2007), produced by the ejection of large dust particles or pebbles from cometary nuclei.

813

814

815

816

817

818

819

820

821

822

Because of its sources of replenishment, the interplanetary dust cloud is not a featureless structure (e. g. Levasseur and Blamont, 1973), although dust particles freshly injected are progressively randomly distributed into the cloud. Whenever interplanetary dust particles impact the atmosphere, they induce the formation of sporadic meteors, meteor showers, or even meteor storms (from fresher dust particles in the cloud) that present a strong temporal and spatial heterogeneity. The flux of entry particles can be tens to hundreds of times higher than during background conditions during the main permanent meteor shower episodes; four main events may be mentioned, the Quadrantids (beginning of January), the Aquarids (beginning of May), the Perseids (mid-August) and the Geminids (mid-December)

823

824

825

826

827

828

829

830

831

832

833

834

As already suspected from comet 1P/Halley flybys in 1986, and established by the Rosetta mission with 67P/Churyumov-Gerasimenko in 2014-2016, the refractory component in comets is rich in high molecular-mass organics, possibly about 45% in mass and 70% in volume (Bardyn et al., 2017; Herique et al., 2017; Levasseur-Regourd et al. 2018); the flux of exogenous material from interplanetary dust entering in the Earth atmosphere is thus rich in complex organics. The dust particles ejected from the nucleus of 67P/Churyumov-Gerasimenko are porous aggregates covering a wide range of sizes, at least from tens to hundreds of μm (Merouane et al., 2016), and of porosities with likely fractal structures (Langevin et al. 2016; Mannel et al. 2016; 2019). Considering the prevalence influx of dust particles originating from JFCs, the speeds of interplanetary dust particles impacting the Earth's atmosphere are mostly low, around 15 km/s range (Nesvorný et al., 2010) or less. Both the relative velocity and the morphology of these porous dust particles should enable



835 the survival of significant amounts of cometary organics within the atmosphere (Levasseur-
836 Regourd and Lasue, 2011).

837 The total amount of material entering the Earth atmosphere is still not well
838 determined, with a daily value in the 5-270 tons range depending of the various techniques
839 used for the determination (Plane, 2012); a mean value of about 100 tons per day is
840 frequently assumed (e.g. Rietmeijer, 1998). Carrillo-Sánchez et al. (2016) have considered
841 the cosmic spherule accretion rate at South Pole, the Na and Fe flux measured in the upper
842 mesosphere coming from the ablation of the incoming solid material, and the satellite
843 measurements of the interplanetary dust cloud radiation. Using ablation-modeling
844 calculations, they have proposed that dust coming from the JFCs contribute to about
845 $80\pm 17\%$ of the dust mass entering the Earth atmosphere estimated at 43 ± 14 tons per day. A
846 large fraction of NSPs commonly *assumed to have a meteoritic origin could in fact originate*
847 *from comets. Thus, it can be suggested* that the aggregated porous and complex organics-
848 rich particles detected in the stratosphere (Ebert et al., 2016; Schutze et al., 2017) could
849 come from comets, not from asteroids, while silicates-rich particles could come either from
850 comets or asteroids.

851 Nevertheless, two difficulties may arise for the detection and the identification of the
852 incoming material and the identification of their origin (cometary dust or meteoroid
853 disintegration in the atmosphere). First, some dust particles may be broken during their
854 atmospheric travel, producing a significant number of smaller particles, some of them being
855 not detectable. Secondly, carbonaceous particles might originate either from space or from
856 Earth. Thus, some layers of concentration enhancements could be produced for particles
857 with similar physically properties as the terrestrial ones but originating from space.

858
859

860 **6. Origin of stratospheric concentration enhancements and transport** 861 **mechanisms**

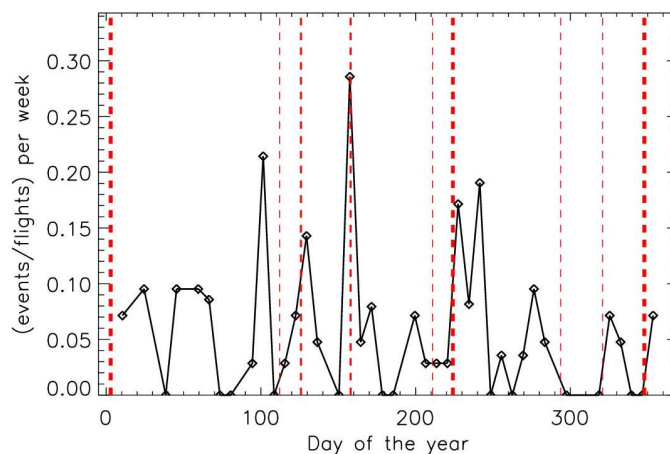
862

863 We discuss here how LOAC particle counter observations under weather balloons
864 could help to better understand the origin and the transport of the NSPs leading to
865 concentration enhancements in the stratosphere.

866 The enhancements reported by various authors were observed sometimes during
867 well-known meteor shower periods but also apart from these events. As said before, about
868 25% of the 135 LOAC and 21 STAC flights exhibit strong enhancements. Such a probability
869 seems to be too high for fortuitous detections of meteoritic disintegrations or of
870 fragmentation of large interplanetary dust.

871 Figure 9 presents the number of concentrations enhancements per flight per week
872 for all the STAC and LOAC balloon flights as a function of the day of the year. The main
873 meteor showers are represented by dotted lines (the thickness of lines is related to the
874 intensity of the episode). No obvious correlation is statistically detected between the
875 variability of the number events and the meteor shower dates and intensities, although
876 some fortuitous coincidence can exist. Then, it can be concluded that the concentrations
877 enhancements in the stratosphere are not directly related to the meteor showers.

878



879
880 *Figure 9: Number of concentrations enhancement per flight per week, for all the LOAC and*
881 *STAC measurements during balloon flights; the red dotted lines represent the main meteor*
882 *showers episodes (the thickness of the dotted lines is related to the intensity of the episode)*
883

884

885 Different dynamical processes may explain the concentration enhancements. A
886 process differing from the common atmospheric transport mechanisms, the gravito-
887 photophoretic effect (Rohatschek, 1996; Pueschel et al., 2000) could allow light-absorbing
888 particles (like BC) to be lifted until the gravity counteracts their ascent, which could explain
889 transport of carbonaceous particles higher up in stratosphere, as for the 2017 Canadian
890 wildfires (Ansmann et al., 2018; Haarig et al., 2018). Such carbonaceous aerosols could stay
891 for several months at the hemispheric scale for these specific events (Kloss et al., 2019) or be
892 present ubiquitously in the tropical lower stratosphere (Murphy et al., 2007; 2014).

893

894 For particles of any nature, as proposed by Beresnev et al. (2012), vertical winds in the
895 stratosphere could be the basic force mechanism rather than gravito-photophoresis for the
896 formation and the spatial and temporal stability of aerosol layers (Gryazin et al., 2011). The
897 vertical winds could provide a levitation of the particles in the stratosphere and could form
898 spatial dynamical traps, in which aerosols are compelled to be in form of thin layers. The
899 averaged vertical wind could be the strong competitor of turbulent diffusion that prevents
900 from the stratification of stratospheric aerosols.

901

902 Another process could provide the levitation and the accumulation layers of soot and
903 BC particles: the radiometric photophoresis effect. Improvements in the theoretical works
904 show that accumulation layers of soot and BC particles could exist at different altitudes in
905 the stratosphere, depending on the size and the shape (compact or fractal) of the particles
906 (Beresnev et al., 2017). The larger the particles are, the potentially higher the accumulation
907 layers could be. In a steady-state atmosphere, accumulation layers of submicronic soot can
908 be in the 10-30 km altitude range; soot aggregates of several micrometers could reach 60 km
909 altitude. But in a non-steady atmosphere, we may expect that these layers are dynamically
910 perturbed and then can disappear.

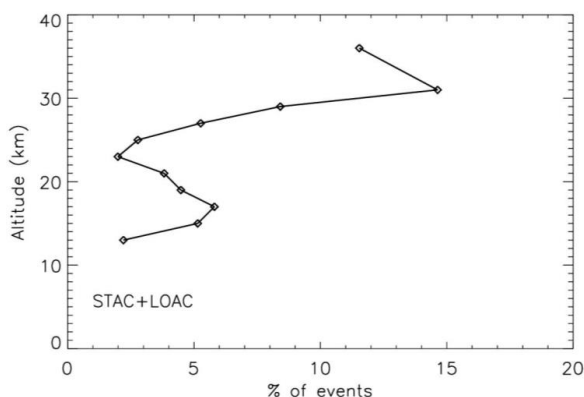
911

912 Finally, strong gravity-wave events could also locally increase the aerosols content
913 and can produce thin layers, as observed one time at mid-latitude with the balloon-borne
914 LOAC (Chane-Ming et al., 2016).



912 Some of these phenomena could explain most of the concentration enhancements
913 attributed to NSPs and previously detected by the STAC balloon-borne aerosols counter at
914 different altitudes and locations (Renard et al., 2008, 2010), and also for the sparse
915 enhancements of carbonaceous particles observed by CALIOP/Calipso during the monsoonal
916 convective season over India (Govardhan et al., 2017). Also, they could explain the enhanced
917 concentrations layers detected after Leonids meteor shower events, linked or not to the
918 disintegration of incoming extraterrestrial material. Soot particles can have different size
919 distributions and fractal/compact shape depending on their origin and their aging (e.g.
920 Adachi et al., 2007), which could explain the various altitudes for the detected accumulation
921 layers.

922 A statistical analysis of the altitude of the concentration enhancement events
923 detected by LOAC seems to indicate a double repartition, one centered at around 17 km and
924 the second one at around 30 km (Figure 10). The analysis is conducted by calculating the
925 percentage of events in respect with the total number of measurements available at the
926 various altitudes. This double repartition looks like the one proposed by Beresnev et al.
927 (2017) for the accumulation layers of fractal and spherical carbonaceous particles
928 respectively (which could correspond to porous fractal aggregates and dense aggregates).
929 The LOAC typologies indicate that optically-absorbing particles dominate the aerosol-
930 enhanced layers although sulfates are also present. The origin of these particles is unknown,
931 since carbonaceous particles coming from space, produced within the atmosphere and
932 emitted from the Earth's surface can be compact and/or fractal.
933



934 *Figure 10: Evolution with altitude of the percentage of concentration enhancement events*
935 *detected by the STAC and LOAC aerosol counters during balloon flights*
936
937

938 939 **7. Background concentrations for large NSPs**

940 Finally, LOAC can be used to estimate the background content of large NSPs, with
941 sizes ranging from several μm up to $100 \mu\text{m}$, usually expected to come from space
942 (interplanetary dust and meteoritic debris), with possible growth by sulfuric acid
943 condensation consequently to their descent in the stratosphere (Bardeen et al., 2008).
944

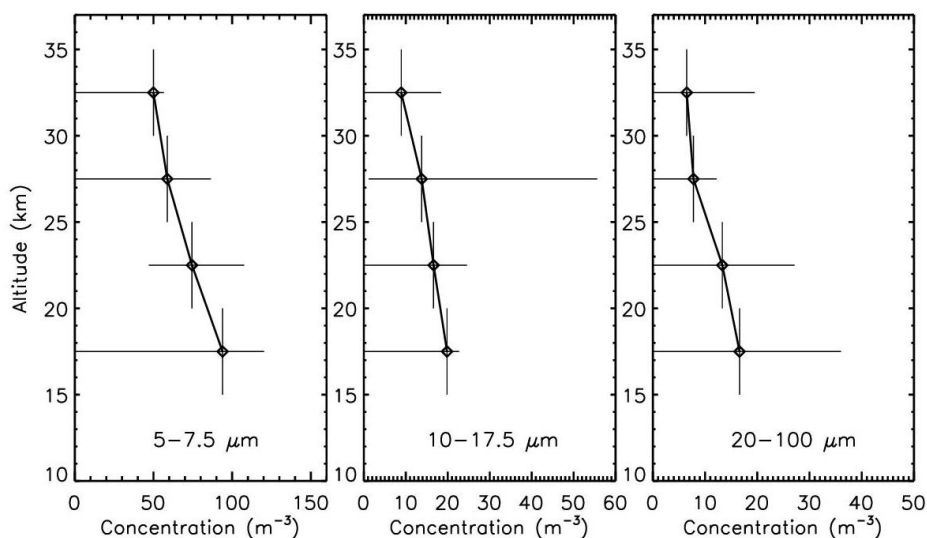
945 Considering the number of flights per year, the balloon ascent speed ($\sim 5 \text{ m}\cdot\text{s}^{-1}$) and
946 the pump flow ($\sim 2 \text{ L}\cdot\text{min}^{-1}$), LOAC has sampled about 1 to 2 m^3 of air per year in the 15-35



947 km altitude range. Figure 11 presents the mean evolution of the concentrations with
948 altitudes of particles detected for the mid-2013 – mid-2019 period, for three size classes (5-
949 7.5 μm , 10-17.5 μm , 20-100 μm) in layers of 5 km width; the error bars represent the
950 interannual variability. The concentrations seem to decrease by about of factor two from 15
951 to 35 km for the three size classes. In the middle stratosphere, the mean concentrations of
952 particles having sizes of about 5 μm , 10 μm and 20 μm are of about 50, 10 and below 10
953 particles m^{-3} , respectively. Although the annual volume of air sampled by LOAC is low, it
954 seems that a tendency could be tentatively pointed out. The lower concentrations values are
955 in the 2017-2018 period (with no particles greater than 10 μm in the middle stratosphere),
956 while the higher concentrations values are in the 2015-2016 period.

957 Ebert et al. (2016) have collected during the RECONCILE campaign inside the polar
958 vortex about 10^3 particles m^{-3} greater than 3 μm in the lower stratosphere (below 21 km).
959 On the other hand, Hunten et al. (1980) using the Brownlee (1978) measurements have
960 estimated the concentration of interplanetary dust (or micrometeorites) at 30 km to be of
961 about 10^{-3} particles m^{-3} for sizes greater than 5 μm . Finally, the concentration of collected
962 particles greater than 5 μm by the DUSTER instrument during one balloon-flight at 38 km
963 was of about one particle m^{-3} (Della Corte et al., 2013). The LOAC estimates cover all these
964 values. Although these sparse measurements have sampled a small volume of the
965 stratospheric air, they could indicate a strong variability for the large particle's
966 concentrations.

967



968

969 *Figure 11: Mean altitude evolutions of the concentrations of the large particles detected by*
970 *LOAC for the 2013-2019 period, for 3 size classes; the errors bars represent the interannual*
971 *variability*

972

973

974

975

976

977

Some of these particles are often classified as “meteoritic material”, based on the presence of Fe, Mg, Ni, Cr, Na in their compositions derived from collected samples or from in situ analysis (Cuicci et al., 2008; Ebert et al., 2016). Interplanetary dust, mainly originated from Jupiter Family Comets, must be also considered. Porous cometary dust particles with



978 not too high relative velocities happen to reach the stratosphere (Levasseur-Regourd et al.,
979 2018) and about 10% of the interplanetary dust flux is likely to reach the Earth's surface
980 without suffering any melting (Dobrica et al., 2010); thus, they can contribute to the
981 carbonaceous particles found in the stratosphere. Nevertheless, we may conclude that the
982 presence of interplanetary material in the stratosphere is dramatically overestimated in the
983 literature, since the detected concentrations are several orders of magnitude above the
984 estimated concentration of material in space at Earth orbit, i. e. 10^{-14} particles cm^{-3} for size
985 greater than $10 \mu\text{m}$ (e. g. Levasseur-Regourd et al., 2001). This last value might be tens or
986 hundreds higher during meteor shower events and even more in case of meteoritic
987 disintegrations inside the stratosphere, but still without reaching the stratospheric
988 concentrations of large NSPs.

989 We can however propose several explanations for these discrepancies:

990 - The flux and the size distribution of incoming material from space is strongly
991 underestimated. In particular, the size distribution estimated from impacts on exposed
992 surfaces in space (Mandeville et al., 1991; Love and Brownlee, 1993; Kalashnikova et al.,
993 2000) could be inaccurate and the retrieved diameters and thus the size distribution could
994 differ from those obtained by optical instruments.

995 - Large fluffy particles (hundreds of μm or greater) entering the Earth atmosphere
996 could undergo breaking processes, producing large number of micron-sized particles and less
997 nanometer-sized (smoke) particles than expected during the ablation processes.

998 - A space-time sampling bias can be assumed. In other words, the dates and the
999 locations of the in situ measurements could be not fully representative of background
1000 conditions, in particular where the regular flights are not well evenly time spaced.

1001 - Some particles produced by the Chelyabinsk meteor disintegration could remain
1002 longer than expected in the stratosphere. This could (partly) explain some high
1003 concentrations values detected by LOAC since the beginning of the measurements in 2013
1004 until the return to lower values at the beginning of 2017; the low concentration of big
1005 particles subsequently to the dilution of the Chelyabinsk meteor cloud in the stratosphere
1006 could be undetectable by spaceborne remote-sensing observations.

1007 - The instruments may have mainly detected material coming from the Earth during
1008 specific events or produced inside the atmosphere and transported to the middle
1009 stratosphere; these particles can remain in some accumulation layers (Beresnev et al., 2012,
1010 2018) and even can agglomerate. We are in favor of this last explanation, since the
1011 concentrations decrease with increasing altitudes, and the accumulation layers were indeed
1012 detected by the STAC and LOAC aerosols counters at the altitude range predicted by the
1013 modelling calculations. Also, the identification of the origin of the particles based on their
1014 composition only could be inaccurate. As an example, the nanocomposites produced inside
1015 the atmosphere (Courty and Martinez, 2015) could have chemical elements like those found
1016 in meteorites or in interplanetary dust.

1017

1018

1019 **5. Conclusions**

1020

1021 Even if a large variety of in situ and remote sensing measurements have been
1022 conducted under different atmospheric conditions, none of them can provide a
1023 comprehensive view describing the whole complexity of the stratospheric NSP content. The
1024 sources are multiple and most of them are non-permanent. One can expect a strong



1025 variability of the chemical composition, the size and the concentration of stratospheric
1026 particles from one session of measurements to another. Also, the particles are likely to be
1027 detected or collected at different stages of their life cycle from their emission to their
1028 removal from the atmosphere during which they are transformed (e.g. condensational
1029 growth, coagulation, inclusion). This complicates the determination of their origin, of their
1030 physical properties and of the processes controlling the evolution of their size distributions
1031 and concentrations.

1032 The LOAC balloon-borne optical counter has contributed to better understand the
1033 origin of the complexity of the NSPs content. It has confirmed the presence of enhanced
1034 layers in terms of concentration of submicronic, and sometimes larger, particles in the lower
1035 and middle stratosphere. The six years of regular flights (2013-2019) have shown a strong
1036 temporal variability of such events, which does not seem to be correlated to the main
1037 meteor shower events. At present, the more plausible hypothesis for such spatial and
1038 temporal behavior is the presence of accumulation layers of terrestrial and atmospheric
1039 particles due to the dynamical and photophoretic effects.

1040 Frequent LOAC balloon flights have shown the necessity to often conduct new
1041 systematic stratospheric measurements at various locations to answer the following open
1042 questions:

- 1043 - How to distinguish between the various sources of particles? How to determine
1044 their average percentages in terms of size, number concentration and mass, and their
1045 evolutions with altitude?
- 1046 - Are there specific physical and chemical markers allowing to distinguish black
1047 carbon and soot particles on a way of formation, types and origins?
- 1048 - Do most of the complex organic particles are coming from space (e. g. cometary
1049 particles) or from the Earth?
- 1050 - Is there an evolution of the physical and chemical properties of the NSPs in the
1051 stratosphere (i.e. aging)?
- 1052 - Is there an increase of the BC/soot particles content in the stratosphere due to
1053 anthropogenic activities especially in Asia?
- 1054 - How long is the residence time of NSPs, depending on their origin and the different
1055 levitation processes involved?
- 1056 - Are the local concentration enhancements really accumulation layers coming from
1057 the vertical winds and photophoretic processes?
- 1058 - Is there a direct link between (charged) NSPs and high-energy phenomena above
1059 thunderstorms?
- 1060 - Finally, what are the consequences of the presence of such particles on Earth's
1061 radiative balance and on the stratospheric chemistry?

1062 Current aerosols counters cannot be used alone to answer these questions, thus new
1063 light instrumentation will be needed, using for instance mass-spectrometers and collecting
1064 devices for frequent and low-cost flights. Also, an optical instrument performing
1065 measurements at several scattering angles could be useful to better evaluate the mean
1066 composition of the particles, as done for example at ground with the laboratory instrument
1067 PROGRA2 (e. g. Hadamcik et al., 2007; Francis et al., 2011). Long-duration balloons flights
1068 from weeks to months with daily vertical excursions and carrying a poly-instrumented
1069 gondola could be also useful to better evaluate the temporal and spatial variability of NSPs
1070 in the stratosphere. Aerosols counter and mass spectrometer can be part of the gondola, but
1071 also a possible future instrument that can derive the isotopic composition of the solid



1072 material to better distinguish between the various sources, as proposed by Kalashnikova et
1073 al., 2016; Beresnev and Vasiljeva, 2018 for carbonaceous particles.

1074 Remote-sensing measurements from future satellite platforms, like the EarthCARE
1075 spaceborne lidar (Illingworth et al., 2015), coupled with balloon-borne measurements, could
1076 help to better identify the various natures of stratospheric aerosols and their variability.
1077 Finally, a new in-situ counting instrument along the Earth's orbit could be proposed to better
1078 estimate the size and the concentration of incoming material from space.

1079 Such improved knowledge of the stratospheric aerosols and the role of the NSPs will
1080 be useful for improving chemistry and climate modeling works, including radiative transfer
1081 calculations over the whole atmosphere.

1082
1083

1084 **Author contribution:** Jean-Baptiste Renard designed the LOAC experiment and processed
1085 the data. Gwenaël Berthet and Damien Vignelles participated in the improvement of the
1086 instrument and of the data processing, and in the data interpretation. Anny-Chantal
1087 Levasseur-Regourd, Sergey Beresnev, Alain Miffre, Patrick Rairoux and Fabrice Jégou
1088 participated in the analysis of the origin of the aerosols and of their spatial and temporal
1089 variability.

1090
1091

1092 **Acknowledgments.** The LOAC instruments were funded by the French Labex “Étude des
1093 géofluides et des VOLatils–Terre, Atmosphère et Interfaces – Ressources et Environnement”
1094 (VOLTAIRE) (ANR-10-LABX-100-01) managed by the University of Orleans. The STAC and
1095 LOAC flights were funded by the French Space Agency CNES. We want to thank the CNES
1096 balloons launching team at Aire sur l’Adour, the MeteoModem Company for the flight for
1097 Ury (France), and Nelson Bègue and the LACy for the flights at Ile de la Réunion. We want to
1098 thank Marie-Agnès Courty for information concerning the local production of
1099 nanocomposite in the atmosphere, Andrei Vedernikov for fruitful discussion, and finally
1100 CNES for its support in the scientific analysis of Rosetta data. Sergey Beresnev want to thank
1101 the Ministry of Science and Higher Education of the Russian Federation, the research project
1102 #3.6064.2017/8.9.

1103

1104 The STAC data are available at:

1105 <https://cds-espri.ipsl.upmc.fr/etherTypo/index.php?id=667&L=1>

1106 The 2013 LOAC data are available at:

1107 http://mistrals.sedoo.fr/?editDatsId=1017&datsId=1017&project_name=ChArMEX

1108 The LOAC data from 2014 are available at:

1109 <https://cds-espri.ipsl.upmc.fr/etherTypo/index.php?id=1699&L=1>

1110
1111

1112 References

1113

1114 Adachi, K., Chung, S. H., Friedrich, H., and Buseck, P. R., Fractal parameters of individual soot
1115 particles determined using electron tomography: implications for optical properties, *J.*
1116 *Geophys. Res.*, 112, D14202, doi:10.1029/2006JD008296, 2007.

1117



- 1118 Ansmann, A., Baars, H., Chudnovsky, A., Mattis, I., Veselovskii, I., Haarig, M., Seifert, P.,
1119 Engelmann, R., and Wandinger, U., Extreme levels of Canadian wildfire smoke in the
1120 stratosphere over central Europe on 21–22 August 2017, *Atmos. Chem. Phys.*, 18, 11831–
1121 11845, 2018.
1122
- 1123 Antonsen, T., Havnes, O., and Mann, I., Estimates of the size distribution of Meteoric smoke
1124 particles from rocket-borne impact probes, *J. Geophys. Res.*, 122, 12,353–12,365.
1125 <https://doi.org/10.1002/2017JD027220>, 2017.
1126
- 1127 Bardeen, C. G., Toon, O. B., Jensen, E. J., Marsh, D. R., and Harvey, V. L., Numerical simulation
1128 of the three-dimensional distribution of meteoric dust in the mesosphere and upper
1129 stratosphere, *J. Geophys. Res.*, 113, D17202, doi:10.1029/2007JD009515, 2008.
1130
- 1131 Bardyn, A., Baklouti, D., Cottin, H., Fray, N., Briois, C., Paquette, J., Stenzel, O., Engrand, C.,
1132 Fischer, H., Hornung, Isnard, R., Langevin, Y., Lehto, H., Le Roy, L., Ligier, N., Merouane, S.,
1133 Modica, P., Orthous-Daunay, F.-R., Rynö, J., Schulz, R., Silén, J., Thirkell, L., Varmuza, K.,
1134 Zaprudin, B., Kissel, J., and Hilchenbach, M., Carbon-rich dust in comet 67P/Churyumov-
1135 Gerasimenko measured by COSIMA/Rosetta, *MNRAS*, 469, S712–S722,
1136 doi.org/10.1093/mnras/stx2640, 2017.
1137
- 1138 Baumgardner, D., Kok, G., and Raga, G., Warming of the Arctic lower stratosphere by light
1139 absorbing particles, *Geophys. Res. Lett.*, 31, L06117, doi:10.129/2003GL0118883, 2004.
1140
- 1141 Bègue, N., Vignelles, D., Berthet, G., Portafaix, T., Payen, G., Jégou, F., Benchérif, H., Jumelet,
1142 J., Vernier, J.-P., Lurton, T., Renard, J.-B., Clarisse, L., Duverger, V., F. Posny, F., Metzger, J.-
1143 M., and Godin-Beekmann, S., Long-range transport of stratospheric aerosols in the Southern
1144 hemisphere following the 2015 Calbuco eruption, *Atmos. Chem. Phys.*, 17, 15019–15036,
1145 2017.
1146
- 1147 Beresnev S., Vasiljeva, M., and Suetin, D. Predictions and detection of the “accommodation”
1148 forces on Janus particles subjected to directed radiation in a rarefied gas, *Vacuum*, 86,
1149 doi:10.1016/j.vacuum.2012.01.022, 1663–1668, 2012.
1150
- 1151 Beresnev, S. A., Vasil’eva, M. S., Gryazin, V. I., and Kochneva, L. B., Photophoresis of fractal-
1152 like soot aggregates: microphysical model, comparison with experiment, and possible
1153 atmospheric manifestations, *atmospheric and oceanic optics*, 30(6), 527–532, doi:
1154 10.1134/S1024856017060045, 2017.
1155
- 1156 Beresnev, S. A., and Vasiljeva, M. S., Black carbon aerosol in stratosphere, *Proc. SPIE 10833*,
1157 24th International Symposium on Atmospheric and Ocean Optics: Atmospheric Physics,
1158 108339D, doi:10.1117/12.2503881, 2018.
1159
- 1160 Berthet, G., Renard, J.-B., Brogniez, C., Robert, C., Chartier, M., and Pirre, M., Optical and
1161 physical properties of stratospheric aerosols from balloon measurements in the visible and
1162 near-infrared domains: 1. Analysis of aerosol extinction spectra from the AMON and
1163 SALOMON balloonborne spectrometers, *Applied Optics*, Vol 41, N° 36, 7522–7539, 2002.
1164



- 1165 Berthet, G., Renard, J.-B., Catoire, V., Chartier, M., Robert, C., Huret, N., Coquelet, F., and
1166 Bourgeois, Q., Remote sensing measurements in the polar vortex: comparison to in situ
1167 observations and implications for the simultaneous retrievals and analysis of the NO₂ and
1168 OCIO species, *J. Geophys. Res.*, Vol.112, D21310, doi:10.1029/2007JD008699, 2007.
1169
- 1170 Bingen, C., Fussen, D., and Vanhellefont, F., A global climatology of stratospheric aerosol
1171 size distribution parameters derived from SAGE II data over the period 1984-2000: 2.
1172 Reference data, *J. Geophys. Res.*, 109, D06202, 2004.
1173
- 1174 Bound, T. C., and Bergstrom, R. W., Light absorption by carbonaceous particles: an
1175 investigative review, *Aerosol Science and Technology*, 40(1), 27-67,
1176 doi.org/10.1080/02786820500421521, 2007.
1177
- 1178 Bourgeois, Q., Ekman, A. M. L., Renard, J.-B., Krejci, R., Devasthale, A., Bender, A.-M.,
1179 Riipinen, I., Berthet, G., and Tackett, J. L., How much of the global aerosol optical depth is
1180 found in the boundary layer and free troposphere, *Atmos. Chem. Phys.*, 18, 7709–7720,
1181 https://doi.org/10.5194/acp-18-7709-2018, 2018.
- 1182
- 1183 Blake, D. F., and Kato, K., Latitudinal distribution of black carbon soot in the upper
1184 troposphere and the lower stratosphere, *J. Geophys. Res.*, 100, 7195-7202, 1995.
1185
- 1186 Bourassa, A. E., Rieger, L. A., Lloyd, N. D., and Degenstein, D. A., Odin-OSIRIS stratospheric
1187 aerosol data product and SAGE III intercomparison, *Atmos. Chem. Phys.*, 12, 605–614,
1188 doi:10.5194/acp-12-605-2012, 2012
1189
- 1190 Brownlee, D. E., *Microparticle studies by sampling techniques*, Cosmic Dust, J. McDonnell
1191 ED., Wiley, 295-336, 1978.
1192
- 1193 Brownlee, D. E., *Cosmic dust: collection and research*, *Ann. Rev. Earth Planet. Sci.*, 13, 147-
1194 173, 1985.
1195
- 1196 Carrillo-Sánchez, J. D., Nesvorný, D., Pokorný, P., Janches, D. and Plane, J. M. C., Sources of
1197 cosmic dust in the Earth's atmosphere, *Geophys. Res. Lett.*, 43, 11,979–11,986, doi:10.1002/
1198 2016GL071697, 2016.
1199
- 1200 Chane-Ming, F., Vignelles, D., Jegou, F., Berthet, G., Renard, J.-B., Gheusi, F., and Kuleshov,
1201 Y., Gravity-wave effects on tracer gases and stratospheric aerosol concentrations during the
1202 2013 ChArMEx campaign, *Atmos. Chem. Phys.*, 16, 8023–8042, doi:10.519/acp-16-8023-
1203 2016, 2016.
1204
- 1205 Ciucci, A., Palumbo, P., Brunetto, R., Della Corte, V., De Angelis, S., Rotundi, A., Rietmeijer,
1206 F.J.M., Zona, E., Colangeli, L., Esposito, F., Mazzotta Epifani, E., Mennella, V., Inarta, S.,
1207 Peterzen, S., Masi, S., and Ibba, R., DUSTER (Dust in the Upper Stratosphere Tracking
1208 Experiment and Retrieval) preliminary analysis, *Memorie della Società Astronomica Italiana*,
1209 75, 282-287, 2008.
1210



- 1211 Coulson, S. G., Wallus, M. K., and Wickramasinghe, N. C., On the dynamics of volatile
1212 meteorites, *Monthly Notices of the Royal Astronomical Society*, 445, 3669-3673, 2014.
1213
- 1214 Courty, M.-A., and Martinez, J.-M., Terrestrial carbonaceous debris tracing atmospheric
1215 hypervelocity-shock aeroplasma processes, *Procedia Engineering*, 103, 81-88, 2015.
1216
- 1217 Curtius, J., Weigel, R., Vossing, H.-J., Wernli, H., Werner, A., Volk, C.M, Konopka, P.,
1218 Krebsbach, M. , Schiller, C. , Roiger, A., Schlager, H., Dreiling, V., and Borrmann, S.,
1219 Observations of meteoric material and implications for aerosol nucleation in the winter
1220 Arctic lower stratosphere derived from in situ particle measurements, *Atmos. Chem. Phys.*,
1221 5, 3053-3069, 2005.
1222
- 1223 Cziczo, D. J., Murphy, D. M., Thomson, D. S., and Ross, M. N., Composition of individual
1224 particles in the wakes of an Athena II rocket and the space shuttle, *Geophys. Res. Lett.*, 29,
1225 21, 2037, doi:10.1029/2002GL015991, 2002.
1226
- 1227 Damoah, R., Spichtinger, N., Servranckx, R., Fromm, M., Eloranta, E. W., Razenkov, I. A.,
1228 James, P., Shulski, M., Forster, C., and Stohl, A., A case study of pyro-convection using
1229 transport model and remote sensing data, *Atmos. Chem. Phys.*, 6, 173-185, 2006.
1230
- 1231 Dartois, E., Engrand, C., Duprat, J., Godard, M., Charon, E., Delauche, L., Sandt, C., and
1232 Borondics, F., Dome C ultracarbonaceous Antarctic micrometeorites. Infrared and raman
1233 fingerprints, *Astron. Astrophys.*, 609, A65, 2018.
1234
- 1235 Della Corte, V., Rietmeijer, F.J.M., Rotundi, A., Ferrari, M., and Palumbo, P., Meteoric CaO
1236 and carbon smoke particles collected in the upper stratosphere from an unanticipated
1237 source, *Tellus B*, 65, 20174, 2013.
1238
- 1239 de Laat, A.T.J., Stein Zweers, D.C., Boers, R., and Tuinder, O.N.E., A solar escalator:
1240 Observational evidence of the self-lifting of smoke and aerosols by absorption of solar
1241 radiation in the February 2009 Australian Black Saturday plume, *J. Geophys. Res.*, 117,
1242 D04204, doi:10.1029/2011JD017016, 2012.
1243
- 1244 Dermott, S.F., Nicholson, P.D., Burns, J.A., and Houck, J.R., On the origin of the IRAS solar
1245 system dust bands, *Nature*, 312, 505-509, 1984.
1246
- 1247 Deshler, T., Hervig, M. E., Hofmann, D. J., Rosen, J. M., and Liley, J. B., Thirty years of in situ
1248 stratospheric aerosol size distribution measurements from Laramie, Wyoming (41°N) using
1249 balloon-borne instruments *J. Geophys. Res.*, 108, D5 4167, doi:10.1029/2002JD002514,
1250 2003.
1251
- 1252 Deshler, T., Richard Anderson-Sprecher, R., Jäger, H., Barnes, J., Hofmann, D. J., Clemesha,
1253 B., Simonich, D., Osborn, M., Grainger, R. G., and Godin-Beekmann, S., Trends in the
1254 nonvolcanic component of stratospheric aerosol over the period 1971–2004, 111, D01201,
1255 10.1029/2005JD006089, 2006.
1256



- 1257 Dobrica, E., Engrand, C., Duprat, J., and Gounelle, M., A statistical overview of concordia
1258 antarctic micrometeorites. *Meteorit. Planet. Sci. Suppl.*, 45, A46, 2010.
1259
- 1260 Ebert, M., Weigel, R., Kandel, K., Günther, G., Molleker, S., Groob, J.-U. Vogel, B., Weinbruch,
1261 S., and Borrmann, S., Chemical analysis of refractory stratospheric aerosol particles collected
1262 within the arctic vortex and inside polar stratospheric clouds, *Atmos. Chem. Phys.* 16, 8405-
1263 8421, 2016.
1264
- 1265 Engrand, C., and Maurette, M., Carbonaceous micrometeorites from Antarctica. *Meteoritics
1266 & Planetary Science* 33:565–580, 1998.
1267
- 1268 Fadnavis, Suvarna, Gayatri Kalita, K. Ravi Kumar, Blaž Gasparini, and Jui-Lin Frank Li,
1269 Potential impact of carbonaceous aerosol on the upper troposphere and lower stratosphere
1270 (UTLS) and precipitation during Asian summer monsoon in a global model simulation, *Atmos.
1271 Chem. Phys.*, 17, 11637–11654, 2017.
1272
- 1273 Flynn, G.J., Wirick, S., and Keller, L.P., Organic grain coatings in primitive interplanetary dust
1274 particles, *Earth Planets Space*, 65, 13, 2013.
1275
- 1276 Fortov, V. E., Sultanov, V. G., and Shutov, A. V., Chelyabinsk superbolide explosion in the
1277 Earth's atmosphere: A common phenomenon or unique coincidence?
1278
- 1279 Francis, M., Renard, J.-B., Hadamcik, E., Couté, B., Gaubicher, B., and Jeannot, M., New
1280 studies on scattering properties of different kinds of soot, *JQSRT*, 112, 1766-1775, 2011.
1281
- 1282 Fromm, M., and R. Servranckx, Transport of forest fire smoke above the tropopause by
1283 supercell convection, *Geophys. Res. Lett.*, 30(10), 1542, doi:10.1029/2002/GL016820, 2003.
1284
- 1285 Fromm, M., Bevilacqua, R., Servranckx, R., Rosen, J., Thayer, J.P., Herman, J., and Larko, D.,
1286 Pyro-cumulonimbus injection of smoke to the stratosphere: Observations and impact of a
1287 super blowup in northwestern Canada on 3–4 August 1998, *J. Geophys. Res.*, 110, D08205,
1288 doi:10.1029/2004JD005350, 2005.
1289
- 1290 Fromm, M., Tupper, A., Rosenfeld, D., Servranckx, R., and McRae, R., Violent pyro-
1291 convective storm devastates Australia's capital and pollutes the stratosphere, *Geophys. Res.
1292 Lett.*, 33, L05815, doi:10.1029/2005GL025161, 2006.
1293
- 1294 Füllekrug, M., Diver, D., Pinçon, J.-L., Phelps, A. D. R., Bourdon, A., Helling, C., Blanc, E.,
1295 Honary, F., Harrison, R. G., Sauvaud, J.-A., Renard, J.-B., Lester, M., Rycroft, M., Kosch, M.,
1296 Horne, R. B., Soula, S., and Gaffet, S., Energetic Charged Particles Above Thunderclouds,
1297 *Surveys in Geophysics*, doi:10.1007/s10712-012-9205-z, 2013.
1298
- 1299 Gao, R. S., Telg, H., McLaughlin, R. J., Ciciora, S. J., Watts, L. A., Richardson, M. S., Schwarz, J.
1300 P., Perring, A. E., Thornberry, T. D., Rollins, A. W., Markovic, M. Z., Bates, T. S., Johnson, J. E.,
1301 and Fahey, D. W., A light-weight, high-sensitivity particle spectrometer for PM2.5 aerosol
1302 measurements, *Aerosol Science and Technology*, 50:1, 88-99, DOI:
1303 10.1080/02786826.2015.1131809, 2016.



- 1304
1305 Gerding, M., Baumgarten, G., Blum, U., Thayer, J. P., Fricke, K.-H., Neuber, R., and Fiedler, J.,
1306 Observation of an unusual mid-stratospheric aerosol layer in the Arctic: possible sources and
1307 implication for polar vortex dynamics (2003), *Ann. Geophys.*, 21, 1057-1069, 2003.
1308
1309 Gorkavyi, N., Rault, D. F., Newman, P. A., da Silva, A. M., and Dudorov, A. E., New
1310 stratospheric dust belt due to the Chelyabinsk bolide, *Geophys. Res. Lett.*, 40, 4728–4733,
1311 doi:10.1002/grl.50788, 2013.
1312
1313 Govardhan, G., Krishnakumari Satheesh, S., Nanjundiah, R., Krishna Moorthy, K., and Suresh
1314 Babu, S., Possible climatic implications of high-altitude black carbon emissions, *Atmos.*
1315 *Chem. Phys.*, 17, 9623-9644, 2017.
1316
1317 Gryazin, V.I., and Beresnev, S.A., Influence of vertical wind on stratospheric aerosol
1318 transport, *Meteorol. Atmos. Phys.*, 110, 151-162, doi: 10.1007/s00703-010-0114-8, 2011.
1319
1320 Günther, A., Höpfner, M., Sinnhuber, B.-M., Griessbach, S., Deshler, T., von Clarmann, T., and
1321 Stiller, G., MIPAS observations of volcanic sulfate aerosol and sulfur dioxide in the
1322 stratosphere, *Atmos. Chem. Phys.*, 18, 1217–1239, 2018.
1323
1324 Hadamcik, E., Renard, J.-B., Lasue, J., Levasseur-Regourd, A.C., Blum, J., and Shraepler, R.,
1325 Light scattering by low density agglomerates of micron-sized grains with the PROGRA2
1326 experiment, *JQSRT*, 106, 74-89, doi.org/10.1016/j.jqsrt.2007.01.008, 2007.
1327
1328 Haarig, M., Ansmann, A., Baars, H., Jimenez, C., Veselovskii, I., Engelmann, R., and Althausen,
1329 D., Depolarization and lidar ratios at 355, 532, and 1064 nm and microphysical properties of
1330 aged tropospheric and stratospheric Canadian wildfire smoke, *Atmos. Chem. Phys.*, 18,
1331 11847–11861, 2018, doi.org/10.5194/acp-18-11847-2018
1332
1333 Hamdan, A., Kabbara, H., Courty, M.-A., Cha, M. S., Martinez, J.-M., and Belmonte, T.,
1334 Synthesis of carbon-metal multi strand nanocomposites by discharges in heptane between
1335 two metallic electrodes, *Plasma Chem. Plasma Process*, 37, 1069-1090, 2017.
1336
1337 Hendricks, J., Kärcher, B., Döpelheuer, A., Feichter, J., Lohmann, U., and Baumgardner, D.,
1338 Simulating the global atmospheric black carbon cycle: A revisit to the contribution of aircraft
1339 emission, *Atmos. Chem. Phys.*, 4, 2521-2541, 2004.
1340
1341 Herique, A., Kofman, W., Beck, P., Bonal, L., Buttarazzi, I., Heggy, E., Lasue, J., Levasseur-
1342 Regourd, A.C., Quirico, E., and Zine, S., Cosmochemical implications of CONSERT permittivity
1343 characterization of 67P/CG, *MNRAS*, 462, S516–S532, doi.org/10.1093/mnras/stx040, 2017.
1344



- 1345 Illingworth, A. J., Barker, H. W., Beljaars, A., Ceccaldi, M., Chepfer, H., Clerbaux, N., Cole, J.,
1346 Delanoë, J., Domenech, C., Donovan, D. P., Fukuda, S., Hiraoka, M., Hogan, R. J.,
1347 Huenerbein, A., Kollias, P., Kubota, T., Nakajima, T., Nakajima, T. Y., Nishizawa, T., Ohno, Y.,
1348 Okamoto, H., Oki, R., Sato, K., Satoh, M., Shephard, M. W., Velázquez-Blázquez, A.,
1349 Wandinger, U., Wehr, T., and Van Zadelhoff, G.-J., The EarthCARE Satellite: The Next Step
1350 Forward in Global Measurements of Clouds, Aerosols, Precipitation, and Radiation, *Bull.*
1351 *American Meteor. Soc.*, 2015, 96 (8), 1311-1332, 2015.
- 1352
1353 Hunten, D. M., Turco, R. P., and Toon, O. B., Smoke and dust particles of meteoric origin in
1354 the mesosphere and stratosphere, *J. Atmos. Sci.*, 37, 1342-1357, 1980.
- 1355
1356 Ishii, H.A., Bradley, J.P., Dai, Z.R., Chi, M., Kearsley, A.T., Burchell, M.J., Browning, N.D., and
1357 Molster, F., Comparison of comet 81P/Wild 2 dust with interplanetary dust from comets,
1358 *Science*, 319, 447, 2008.
- 1359
1360 Jégou, F., Berthet, G., Brogniez, C., Renard, J.-B., Francois, P., Haywood, J. M., Jones, A.,
1361 Bourgeois, Q., Lurton, T., Auriol, F., Godin-Beekmann, S., Guimbaud, C., Krysztofiak, G.,
1362 Gaubicher, B., Chartier, M., Clarisse, L., Clerbaux, C., Balois, J.-Y., Verwaerde, C., and D.
1363 Daugeron, Stratospheric aerosols from the Sarychev volcano eruption in the 2009 Arctic
1364 summer, *Atmos. Chem. Phys.*, 13, 6533–6552, 2013, doi:10.5194/acp-13-6533-2013, 2013.
- 1365
1366 Jessberger, E.K., Stephan, T., Rost, D., Arndt, P., Maetz, M., Stadermann, F.J., Brownlee, D.E.,
1367 Bradley, J.P., and Kurat, G., Properties of interplanetary dust: Information from collected
1368 samples, In: *Interplanetary Dust* (Grün, E., Gustafson, B.A.S, Dermott, S.F., and Fichtig, H.,
1369 Eds), Springer-Verlag, Berlin, 253-294, 2001.
- 1370
1371 Jost, H.-J., Drdla, K., Stohl, A., Pfister, L., Loewenstein, M., Lopez, J. P., Hudson, P. K., Murphy,
1372 D. M., Cziczo, D. J., Fromm, M., Bui, T. P., Dean-Day, J., Gerbig, C., Mahoney, M. J., Richard, E.
1373 C., Spichtinger, N., Vellovic Pittman, J., Weinstock, E., M., Wilson, J., and Xueref, I., In-situ
1374 observations of mid-latitude forest fire plumes deep in the stratosphere, *Geophys. Res. Lett.*,
1375 31, doi:10.1029/2003GL019253, 2004.
- 1376
1377 Kalashnikova, O., Horanyi, M., Thomas, G. E., and Toon, O. B., Meteoric smoke production in
1378 the atmosphere, *Geophys. Res. Lett.*, 27(20), 3293-3296, 2000.
- 1379
1380 Kalashnikova, D.A., Markelova, A.N., Melkov, V.N., and Simonova, G.V., Isotope composition
1381 of pyrogenic carbon of various origins, *Chem. Sustain. Develop.* 24, 467–471, 2016.
- 1382
1383 Khaykin, Sergey M., Sophie Godin-Beekmann, Philippe Keckhut, Alain Hauchecorne, Julien
1384 Jumelet, Jean-Paul Vernier, Adam Bourassa, Doug A. Degenstein, Landon A. Rieger, Christine
1385 Bingen, Filip Vanhellemont, Charles Robert, Matthew DeLand, and Pawan K. Bhartia,
1386 Variability and evolution of the midlatitude stratospheric aerosol budget from 22 years of
1387 ground-based lidar and satellite observations, *Atmos. Chem. Phys.*, 17, 1829–1845, 2017.
- 1388
1389 Khaykin, S. M., Godin-Beekmann, S., Hauchecorne, A., Pelon, J., Ravetta, F., and Keckhut, P.,
1390 Stratospheric smoke with unprecedentedly high backscatter observed by lidars above
1391 southern France, *Geophys. Res. Lett.*, 1944, 8007, doi:10.1002/2017GL076763, 2018.



- 1392
1393 Klekociuk, A., Brown, P. G., Pack, D. W., ReVelle, D. O., Edwards, W. N., Spalding, R. E.,
1394 Tagliaferri, E., Yoo, B., B., and Zagari, J., Meteoritic dust from the atmospheric disintegration
1395 of a large meteoroid, *Nature*, 436, doi:10.1038/nature03881, 2005.
1396
1397 Kloss, C., Berthet, G., Sellitto, P., Ploeger, F., Bucci, S., Khaykin, S., Jégou, F., Taha, G.,
1398 Thomason, L., Barret, B., Le Flochmoen, E., von Hobe, M., Bossolasco, A., Begue, N., and
1399 Legras, B., Transport of the 2017 Canadian wildfire plume to the tropics and global
1400 stratosphere via the Asian monsoon circulation, *ACP Discussions*,
1401 <https://doi.org/10.5194/acp-2019-204>, 2019.
1402
1403 Koschny, D., Soja, R., Engrand, C., Flynn, G., Lasue, J., Levasseur-Regourd, A. C., Malaspina,
1404 D., Nakamura, T., Poppe, A. R., Sterken, V. J., and Trigo-Rodríguez, J. M., *Space Science*
1405 *Reviews*, 215-34, doi.org/10.1007/s11214-019-0597-7, 2019.
1406
1407 Kremser, S., Thomason, L. W., von Hobe, M., Hermann, M., Deshler, T., Timmreck, C.,
1408 Toohey, M., Stenke, A., Schwarz, J. P., Weigel, R., Fueglistaler, S., Prata, F. J., Vernier, J.-P.,
1409 Schlager, H., Barnes, J. E., Antuña-Marrero, J.-C., Fairlie, D., Palm, M., Mahieu, E., Notholt, J.,
1410 Rex, M., Bingen, C., Vanhellemont, F., Bourassa, A., Plane, J. M. C., Klocke, D., Carn, S. A.,
1411 Clarisse, L., Trickl, T., Neely, R., James, A. D., Rieger, L., Wilson, J. C., and Meland, B.,
1412 Stratospheric aerosol – Observations, processes, and impact on climate, *Rev. Geophys.*, 54,
1413 278–335, 2016.
1414
1415 Langevin, Y., Hilchenbach, M., Ligier, N., Merouane, S., Hornung, K., Engrand, C., Schulz, R.,
1416 Kissel, J., Rynö, J., and Eng, P., Typology of dust particles collected by the COSIMA mass
1417 spectrometer in the inner coma of 67P/Churyumov-Gerasimenko, *Icarus*, 271, 76-97, 2016.
1418
1419 Lasue, J., Levasseur-Regourd, A.C., Fray, N., and Cottin, H. Inferring the interplanetary dust
1420 properties from remote observations and simulations, *Astronomy & Astrophysics*, 473, 641-
1421 649, doi: 10.1051/0004-6361:20077623, 2007.
1422
1423 Levasseur, A.C., and Blamont, J.E., Satellite observations of intensity variations of the
1424 zodiacal light, *Nature*, 246, 5427, 26-28, 1973.
1425
1426 Levasseur-Regourd A.C., Mann, I., Dumont, R., and Hanner, M.S., Optical and thermal
1427 properties of interplanetary dust. In: *Interplanetary Dust* (Grün, E., Gustafson, B.A.S,
1428 Dermott, S.F., and Fechtig, H., Eds), Springer-Verlag, Berlin, 57-94, 2001.
1429
1430 Levasseur-Regourd, A.C., and Lasue, J., Inferring sources in the interplanetary dust cloud,
1431 from observations and simulations of zodiacal light and thermal emission, In *Meteoroids: the*
1432 *smallest solar system bodies*, NASA/CP-2011-216469, 66-75, 2011.
1433
1434 Levasseur-Regourd, A.C., Agarwal, J., Cottin, H., Engrand, C., Flynn, G., Fulle, M., Gombosi, T.,
1435 Langevin, Y., Lasue, J., Mannel, T., Merouane, S., Poch, O., Thomas, N., and Westphal, A.,
1436 Cometary dust, *Space Sci. Rev.*, 214, 64-119, doi.org/10.1007/s11214-018-0496-3, 2018.
1437



- 1438 Love, S., and Brownlee, D., A direct measurement of the terrestrial mass accretion rate of
1439 cosmic dust, *Science* 262, 54-58, 1993.
- 1440
- 1441 Lurton, T., Renard, J.-B., Vignelles, D., Jeannot, M., Akiki, R., Mineau, J.-L., and Tonnelier, T.,
1442 Light scattering at small angles by atmospheric irregular particles: modelling and laboratory
1443 measurements, *Atmospheric Measurement Techniques*, *Atmos. Meas. Tech.*, 7, 931–939,
1444 2014.
- 1445
- 1446 Mannel, T., Bentley, M.S., Schmied, R., Jeszenszky, H., Levasseur-Regourd, A.C., Romstedt, J.,
1447 and Torkar, K., Fractal cometary dust: a window into the early Solar System, *MNRAS*, 462,
1448 S304-S311, doi.org/10.1093/mnras/stw2898, 2016.
- 1449
- 1450 Mannel, T., Bentley, M. S., Boakes, P., Jeszenszky, H., Ehrenfreund, P., Engrand, C., Koeberl,
1451 C., Levasseur-Regourd, A. C., Romstedt, J., Schmied R., Torkar K., and Weber, I.
1452 *Astronomy and Astrophysics*, 2019, 630, A26 (14 p.), doi.org/10.1051/0004-
1453 6361/201834851, 2019.
- 1454
- 1455 Mateshvili, N., Mateshvili, G., Mateshvili, I., Gheondjian, L., and Avsajanishvili, Vertical
1456 distribution of dust particles in the Earth's atmosphere during the 1998 Leonids, *Meteoritics
1457 B Planetary Science* 34, 969-913, 1999.
- 1458
- 1459 Mandeville, J.-C., Study of cosmic dust particles on board LDEF and MIR space station, *Origin
1460 and Evolution of interplanetary dust*, A.C. Levasseur-Regourd and H. Hasegawa eds., Kluwer
1461 Academic Publishers, 11-14, 1991.
- 1462
- 1463 Merouane, S., Zaprudin, B., Stenzel, O., Langevin, Y., Altobelli, N., Della Corte, V., Fischer, H.,
1464 Fulle, M., Hornung, K., Silén, J., Ligier, N., Rotundi, A., Ryno, J., Schulz, R., Hilchenbach, M.,
1465 Kissel, J., and the COSIMA Team, Dust particle flux and size distribution in the coma of
1466 67P/Churyumov-Gerasimenko measured in situ by the COSIMA instrument on board
1467 Rosetta, *A&A* 596, A87, 2016.
- 1468
- 1469 Mishchenko, M.I., Hovenier, J. W., and Mackowski, D. W., Single scattering by a small volume
1470 element, *J. Opt. Soc. Amer. A*, 21, 71-87, doi:10.1364/JOSAA.21.000071, 2004.
- 1471
- 1472 Miffre, A., Anselmo, C., Geffroy, S., Fréjafon, E., and Rairoux, P., Lidar remote sensing of
1473 laser-induced incandescence on light absorbing particles in the atmosphere, *Optics Express*,
1474 23 (3), 2347-2360, 2015.
- 1475
- 1476 Murphy, D. M., Thomson, D. S., and Mahoney, M. J., In situ measurements of organics,
1477 meteoritic material, mercury, and other elements in aerosols at 5 to 19 kilometers, *Science*,
1478 282, 1664-1669, 1998.
- 1479
- 1480 Murphy, D. M., Cziczo, D. J., Hudson, P. K., and Thomson, D. S., Carbonaceous material in
1481 aerosol particles in the lower stratosphere and tropopause region, *J. Geophys. Res.*, 112,
1482 D04203, doi:10.1029/2006JD007297, 2007.
- 1483



- 1484 Murphy, D. M., Froyd, K. D., Schwarz, J. P., and Wilson, J. C., observation of the chemical
1485 composition of stratospheric aerosol particles, *Q. J. R. Meteorol. Soc.*, 140, 1269-1278, 2014.
1486
- 1487 Nakamura, T., Noguchi, T., Ozono, Y., Osawa, T., and Nagao, K., Mineralogy of
1488 ultracarbonaceous large micrometeorites, *Meteorit. Planet. Sci.*, 40 (Suppl), 5046, 2005.
1489
- 1490 Neely, R. R., J. M. English, O. B. Toon, S. Solomon, M. Mills, and J. P. Thayer, Implications of
1491 extinction due to meteoritic smoke in the upper stratosphere, *Geophys. Res. Lett.* 38,
1492 L24808, doi:10.1029/2011GL049865, 2011.
1493
- 1494 Nesvorný, D., Jenniskens, P., Levison, H.F., Bottke, W.F., Vokrouhlicky, D., and Gounelle, M.,
1495 Cometary origin of the zodiacal cloud and carbonaceous micrometeorites: Implications for
1496 hot debris disks, *The Astrophysical Journal*, 713, 816-836, 2010.
1497
- 1498 Newman, P.A., Wilson, J.C., Ross, M.N., Brock, C.A., Sheridan, P.J., Schoeberl, M.R., Lait, L.R.,
1499 Bui, T.P., Loewenstein, M., and Podolske, J.R., Chance encounter with a stratospheric
1500 kerosene rocket plume from Russia over California. *Geophys. Res. Lett.* 28 (6), 959–962,
1501 2001.
1502
- 1503 Niemeier, U., Timmreck, C., Graf, H.-F., Kinne, S., Rast, S., and Self, S., Initial fate of fine ash
1504 and sulfur from large volcanic eruption, *Atmos. Chem. Phys.*, 9, 9043-9057, 2009
1505
- 1506 Padma Kumari, B., Trigo-Rodriguez, J. M., Londhe, A. L., Jadhav, D. B., and Trimbake, H. K.,
1507 Optical observations of meteoric dust in the middle stratosphere during Leonid activity in
1508 recent years 2001-2003 over India, *Geophys. Res. Lett.*, 32, L16807,
1509 doi:10.1029/2005GL023434, 2005.
1510
- 1511 Padma Kumari, B., Kulkarni, H., Jadhav, D. B., Londhe, A. L., and Trimbake, H. K., Exploring
1512 Atmospheric aerosols by twilight photometry, *Journal of Atmospheric and Oceanic*
1513 *Technology*, 25, 1600-1607, 2008.
1514
- 1515 Pereira, J., Massereau-Guilbaud, V., Géraud-Grenier, I., and Plain, A., CH and CN radical
1516 contribution in the particle formation generated in a radio-frequency CH₄/N₂ plasma,
1517 *Plasma Process. Polym.*, 2, 633–640 DOI: 10.1002/ppap.200500014, 2005.
1518
- 1519 Peterson D. A., Campbell, J. R., Hyer, E. J., Fromm, M. D., Kablick III, G. P., Cossuth, J. H., and
1520 DeLand, M. T., Wildfire-driven thunderstorms cause a volcano-like stratospheric injection of
1521 smoke. *npj Climate and Atmospheric Science* 1:2397–3722, 2018.
1522
- 1523 Plane, J. M. C., Atmospheric chemistry of meteoric metals, *Chem. Rev.*, 103, 4963-4984,
1524 2003.
1525
- 1526 Plane, J. M. C., Cosmic dust in the earth's atmosphere, *Chem. Soc. Rev.*, 41, 6507-6518,
1527 2012.
1528



- 1529 Plane, J. M. C., Flynn, G. J., Määttänen, A., Moores, J. E., Poppe, A. R., Carrillo-Sanchez, J. D.,
1530 and Listowsky, C., Impacts of cosmic dust on planetary atmospheres and surfaces, *Space Sci.*
1531 *Rev.*, 214:23, <https://doi.org/10.1007/s11214-017-0458-1>, 2018.
- 1532
- 1533 Pueschel, R. F., Black, D. F., Snetsinger, K. G., Hansen, A. D. A., Verma, S., and Kato, K., Black
1534 carbon (soot) in the lower stratosphere and upper troposphere, *Geophys. Res. Lett.*, 19(16),
1535 1659-1662, 1992.
- 1536
- 1537 Pueschel, R.F., Boering, K.A., Verma, S., Howard, S.D., Ferry, G.V., Goodman, J., Allen, D.A.,
1538 and Hamil, P., Soot aerosol in the lower stratosphere: Pole-to-pole variability and
1539 contributions by aircraft, *J. Geophys. Res.*, 102, D11, 13,113-13,118, 1997.
- 1540
- 1541 Pueschel, R. F., Verma, S., Rohatschek, H., Ferry, G. V., Boiadjieva, N., Howard, S. D., and
1542 Strawa, A. W., Vertical transport of anthropogenic soot aerosol into the middle atmosphere,
1543 *J. Geophys. Res.*, 105, 3727-3736, 2000.
- 1544
- 1545 Rapp, M., Strellnikova, I., and Gumbel, J., Meteoric smoke particles: Evidence from rocket
1546 and radar techniques, *Adv. Space Res.*, 40., 809-817, 2007.
- 1547
- 1548 Reach, W.T., Kelley, M.S., and Sykes, M.V., A survey of debris trails from short-period
1549 comets. *Icarus*, 191, 298-322, 2007.
- 1550
- 1551 Renard, J.-B., Berthet, G., Robert, C., Chartier, M., Pirre, M., Brogniez, C., Herman, M.,
1552 Verwaerde, C., Balois, J.-Y., Ovarlez, J., Ovarlez, H., Crespin, J., and Deshler, T., Optical and
1553 physical properties of stratospheric aerosols from balloon measurements in the visible and
1554 near-infrared domains : 2. Comparison of extinction, reflectance, polarization and counting
1555 measurements, *Applied Optics*, Vol 41, N° 36, 7540-7549, 2002.
- 1556
- 1557 Renard, J.-B., Ovarlez, J., Berthet, G., Fussen, D., Vanhellemont, F., Brogniez, C., Hadamcik,
1558 E., Chartier, M., and Ovarlez, H., Optical and physical properties of stratospheric aerosols
1559 from balloon measurements in the visible and near-infrared domains. III. Presence of
1560 aerosols in the middle stratosphere, *Applied Optics*, vol. 44, N° 19, 4086-4095, 2005.
- 1561
- 1562 Renard, J.-B., Brogniez, C., Berthet, G., Bourgeois, Q., Gaubicher, B., Chartier, M., Balois, J.-Y.
1563 Verwaerde, C., Auriol, F., Francois, P., Dageron, D., and Engrand, C., Vertical distribution of
1564 the different types of aerosols in the stratosphere, Detection of solid particles and analysis
1565 of their spatial variability, *J. Geophys. Res.*, 113, D21303, doi:10.1029/2008JD010150, 2008.
- 1566
- 1567 Renard, J.-B., Berthet, G., Salazar, V., Catoire, V., Tagger, M., Gaubicher, B., and Robert, C., In
1568 situ detection of aerosol layers in the middle stratosphere, *Geophys. Res. Lett.*, 37, L20803,
1569 doi:10.1029/2010GL044307, 2010.
- 1570
- 1571 Renard, J.-B., Tripathi, S. N., Michael, M., Rawal, A., Berthet, G., Fullekrug, M., Harrison, R.
1572 G., Robert, C., Tagger, M., and Gaubicher, B., In situ detection of electrified aerosols in the
1573 upper troposphere and stratosphere, *Atmos. Chem. Phys.*, 13, 11187–11194, 2013,
1574 doi:10.5194/acp-13-11187-2013.
- 1575



- 1576 Renard, J.-B., Dulac, F., Berthet, G., Lurton, T., Vignelles, D., Jégou, F., Tonnelier, T., Jeannot,
1577 M., Couté, B., Akiki, R., Verdier, N., Mallet, M., Gensdarmes, F., Charpentier, P., Mesmin, S.,
1578 Duverger, V., Dupont, J.-C., Elias, T., Crenn, V., Sciare, J., Zieger, P., Salter, M., Roberts, T.,
1579 Giacomoni, J., Gobbi, M., Hamonou, E., Olafsson, H., Dagsson-Waldhauserova, P., Camy-
1580 Peyret, C., Mazel, C., Décamps, T., Piringer, M., Surcin, J., and Daugeron, D.: LOAC, a light
1581 aerosols counter for ground-based and balloon measurements of the size distribution and of
1582 the main nature of atmospheric particles, 1. Principle of measurements and instrument
1583 evaluation, *Atmos. Meas. Tech.*, 9, 1721-1742, doi:10.5194/amt-9-1721-2016, 2016a.
1584
1585 Renard, J.-B., Dulac, F., Berthet, G., Lurton, T., Vignelles, D., Jégou, F., Tonnelier, T., Jeannot,
1586 M., Couté, B., Akiki, R., Verdier, N., Mallet, M., Gensdarmes, F., Charpentier, P., Mesmin, S.,
1587 Duverger, V., Dupont, J.-C., Elias, T., Crenn, V., Sciare, J., Zieger, P., Salter, M., Roberts, T.,
1588 Giacomoni, J., Gobbi, M., Hamonou, E., Olafsson, H., Dagsson-Waldhauserova, P., Camy-
1589 Peyret, C., Mazel, C., Décamps, T., Piringer, M., Surcin, J., and Daugeron, D.: LOAC, a light
1590 aerosols counter for ground-based and balloon measurements of the size distribution and of
1591 the main nature of atmospheric particles, 2. First results from balloon and unmanned aerial
1592 vehicle flights, *Atmos. Meas. Tech.*, 9, 3673-3686, doi:10.5194/amt-9-3673-2016, 2016b.
1593
1594 Renard, J.-B., Dulac, F., Durand, P., Bourgeois, Q., Denjean, C., Vignelles, D., Couté, B.,
1595 Jeannot, M., Verdier, N., and Mallet, M., In situ measurements of desert dust particles above
1596 the western Mediterranean Sea with the balloon-borne Light Optical Aerosol Counter/sizer
1597 (LOAC) during the ChArMEx campaign of summer 2013, *Atmos. Chem. Phys.*, 18, 3677-3699,
1598 <http://doi.org/10.5194/acp-18-3677-2018>, 2018.
1599
1600 Rieger, L. A., Bourassa, A. E., and Degenstein, D. A., Odin-OSITIS detection of the Chelyabinsk
1601 meteor, *Atmos. Meas. Tech.*, 7, 777-780, doi:10.5194/amt7-777-2014, 2014.
1602
1603 Rietmeijer, F.J.M., Interplanetary dust particles, *Reviews in mineralogy*, 36, 1-96, 1998.
1604
1605 Rohatschek, H., Levitation of stratospheric and mesospheric aerosols by gravito-
1606 photophoresis, *J. Aerosol Sci.*, 27, 467-475, 1996.
1607
1608 Ross, M. N., Whitefield, P. D., Hagen, D. E., and Hopkins, A. R., In situ measurement of the
1609 aerosol size distribution in stratospheric solid rocket motor exhaust plumes. *Geophys. Res.*
1610 *Lett.* 26(7), 819-822, 1999.
1611
1612 Rowan-Robinson, M., and May, B., An improved model for the infrared emission from the
1613 zodiacal dust cloud: cometary, asteroidal and interstellar dust, *MNRAS*, 429, 2894-2902,
1614 doi:10.1093/mnras/sts471, 2013.
1615
1616 Russell, P. B., Livingston, J. M., Pueschel, R. F., Bauman, J. J., Pollack, J. B., Brooks, S. L.,
1617 Hamill, P., Thomason, L. W., Stowe, L. L., Deshler, T., Dutton, E. G., and Bergstrom, R. W.,
1618 Global to microscale evolution of the Pinatubo volcanic aerosol derived from diverse
1619 measurements and analyses *J. Geophys. Res.*, 101, 18745-18763, 1996.
1620
1621 Salazar, V., Renard, J.-B., Hauchecorne, A., Bekki, S., and Berthet, G., A new climatology of
1622 aerosols in the middle and upper stratosphere by alternative analysis of GOMOS



- 1623 observations during 2002–2006, *International Journal of Remote Sensing*, Volume 34, Issue
1624 14, 4986-5029, doi: 10.1080/01431161.2013.786196, 2013.
- 1625
- 1626 Sandford, S. A., Engrand, C., and Rotundi, A., *Organic Matter in Cosmic Dust*, *Elements*, 12,
1627 185-189, 2016.
- 1628
- 1629 Schwarz, J. P., Gao, R. S., Fahey, D. W., Thomson, D. S., Watts, L. A., Wilson, J. C., Reeves, J.
1630 M., Darbeheshti, M., Baumgardner, D. G., Kok, G. L., Chung, S. H., Schulz, M., Hendricks, J.,
1631 Lauer, A., Kärcher, B., Slowik, J. G., Rosenlof, K. H., Thompson, T. L., Langford, A. O.,
1632 Loewenstein, M., and Aikin, K. C., Single-particle measurements of mid-latitude black carbon
1633 and light-scattering aerosols from the boundary layer to the lower stratosphere, *J. Geophys.*
1634 *Res.*, 111, D16207, doi:10.1029/2006JD007076, 2006.
- 1635
- 1636 Schütze, K., Wilson, J.C., Weinbruch, S., Benker, N., Ebert, M., Günther, G., Weigel, R., and
1637 Borrmann, S., Sub-micrometer refractory carbonaceous particles in the polar stratosphere,
1638 *Atmos. Chem. Phys.* 17, 12475-12493, 2017.
- 1639
- 1640 Scott J. D., and Chittenden II, D. M., Chemical composition of particles of $d < 0.20 \mu$ in the
1641 lower stratospheric aerosol, Spring 1993, *Journal of the Arkansas Academy of Science*, 56 23,
1642 2002.
- 1643
- 1644 Sheng, J.-X., Weisenstein, D. K., Luo, B.-P., Rozanov, E., Stenke, A., Anet, J., Bingemer, H., and
1645 Peter, T., Global atmospheric sulfur budget under volcanically quiescent conditions: Aerosol-
1646 chemistry-climate model predictions and validation, *J. Geophys. Res. Atmos.*, 120, 256–276,
1647 doi:10.1002/2014JD021985, 2015.
- 1648
- 1649 Siebert, J., Timmis, C., Vaughan, G., and Fricke, K.H., A strange cloud in the Arctic summer
1650 stratosphere 1998 above Esrange (68°N), Sweden, *Ann. Geophysicae* 18, 505-509, 2000.
- 1651
- 1652 Solomon, S., Daniel, J. S., Nelly, R. R., Vernier, J.-P., Dutton, E. G., and Thomason, L. W., The
1653 persistently variable "background" stratospheric aerosol layer and global climate change,
1654 *Science*, 333(6044), 866-870, 2011.
- 1655
- 1656 Stein, B., Del Guasta, M., Kolenda, J., Morandi, M., Rairoux, P., Stefanutti, L., Wolf, J. P., and
1657 Wöste, L., Stratospheric aerosol size distributions from multispectral lidar measurements at
1658 Sodankylä during EASOE, *Geophys. Res. Lett.*, 21 (13), 1311-1314, 1994.
- 1659
- 1660 Strawa, A. W., Drdla, K., Ferry, G. V., Verma, S., Pueschel, R. F., Yasuda, M., Salawitch, R. J.,
1661 Gao, R. S., Howard, S. D., Bui, P. T., Loewenstein, M., Elkins, J. W., Perkins, K. K., and Cohen,
1662 R., Carbonaceous aerosol (soot) measured in the lower stratosphere during POLARIS and its
1663 role in stratospheric photochemistry, *J. Geophys. Res.*, 104, 26,753-26,766, 1999.
- 1664
- 1665 Sykes, M.V., Hunten, D.M., and Low, F.J., Preliminary analysis of cometary dust trails, *Adv.*
1666 *Space Res.*, 6, 67-78, 1986.
- 1667



- 1668 Testa Jr., J. P., Stephens, J. R., Berg, W. W., Cahill, T. A., Onaka, T., Nakada, Y., Arnold, J. R.,
1669 Fong, N., and Sperry P. D., Collection of microparticles at high balloon altitudes in the
1670 stratosphere, *Earth and Planetary Science Letters*, 98, (3–4), 287-302, 1990.
- 1671
1672 Thomas K. L., Blanford, G. E., Keller, L. P., Klöck, W., and McKay, D., Carbon abundance and
1673 silicate mineralogy of anhydrous interplanetary dust particles, *Geochim. Cosmochim. Acta*,
1674 57, 1551-1566, 1993.
- 1675 Thomason, L. W., Ernest, N., Millán, L., Rieger, L., Bourassa, A., Vernier, J.-P., Manney, G.,
1676 Luo, B., Arfeuille, F., and Peter, T., A global space-based stratospheric aerosol climatology
1677 1979-2016, *Earth Syst. Sci. Data*, 10, 469–492, 2018 [https://doi.org/10.5194/essd-10-469-](https://doi.org/10.5194/essd-10-469-2018)
1678 2018, 2018.
- 1679
1680 Vanhellefont, F., Fussen, D., Mateshvili, N., Tétard, C., Bingen, C., Dekemper, E., Loodts, N.,
1681 Kyrölä, E., Sofieva, V., Tamminen, J., Hauchecorne, A., Bertaux, J.-L., Dalaudier, F., Blanot, L.,
1682 Fanton d’Andon, O., Barrot, G., Guirlet, M., Fehr, T., and L. Saavedra, Optical extinction by
1683 upper tropospheric/ stratospheric aerosols and clouds: GOMOS observations for the period
1684 2002-2008, *Atmos. Chem. Phys.*, 10, 7997–8009 www.atmos-chem-phys.net/10/7997/2010/
1685 [doi:10.5194/acp-10-7997-2010](https://doi.org/10.5194/acp-10-7997-2010), 2010.
- 1686
1687 Vernier, J. P., Pommereau, J.-P., Garnier, A., Pelon, J., Larsen, N., Nielsen, J., Christensen, T.,
1688 Cairo, F., Thomason, L. W., Leblanc, T., and McDermid, I. S., Tropical stratospheric aerosol
1689 layer from CALIPSO lidar observations, *J. Geophys. Res.*, 114, D00H10,
1690 [doi:10.1029/2009JD011946](https://doi.org/10.1029/2009JD011946), 2009.
- 1691
1692 Vernier, J.-P., Thomason, L. W., Pommereau, J.-P., Bourassa, A., Pelon, J., Garnier, A.,
1693 Hauchecorne, A., Blanot, L., Trepte, C., Degenstein, D., and Vargas, F., Major influence of
1694 tropical volcanic eruptions on the stratospheric aerosol layer during the last decade,
1695 *Geophys. Res. Lett.*, 38, L12807, [doi:10.1029/2011GL047563](https://doi.org/10.1029/2011GL047563), 2011.
- 1696
1697 Vernier, J. P., Fairlie, T. D., Deshler, T., Natarajan, M., Knepp, T., Foster, K., Wienhold, F. G.,
1698 Bedka, K. M., Thomason, L. W., and Trepte, C., In situ and space observations of the Kelud
1699 volcanic plume: the persistence of ash in the lower stratosphere, *J. Geophys. Res., Atmos.*,
1700 121, 11,104-11,118, [doi:10.1002/2016JD025344](https://doi.org/10.1002/2016JD025344), 2016.
- 1701
1702 Vernier, J.-P., Fairlie, T. D., Deshler, T., Venkat Ratnam, M., Gadhavi, H., Kumar, B. S.,
1703 Natarajan, M., Pandit, A. K., Akhil Raj, S. T., Hemanth Kumar, A., Jayaraman, A., Singh, A. K.,
1704 Rastogi, N., Sinha, P. R., Kumar, S., Tiwari Banaras, S., Wegner, T., Baker, N., Vignelles, D.,
1705 Stenchikov, G., Shevchenko, I., Smith, J., Bedka, K., Kesarkar, A., Singh, V., Bhate, J.,
1706 Ravikiran, V., Durga Rao, M., Ravindrababu, S., Patel, A., Vernier, H., Wienhold, F. G., Liu, H.,
1707 Knepp, T. N., Thomason, L., Crawford, J., Ziemba, L., Moore, J., Crumeyrolle, S., Williamson,
1708 M., Berthet, G., Jégou, F., and Renard, J.-B., BATAL: The Balloon Measurement Campaigns of
1709 the Asian Tropopause Aerosol Layer, *Bulletin of the American Meteorological Society*, 99 (5),
1710 955-973, [doi:10.1175/BAMS-D-17-0014.1](https://doi.org/10.1175/BAMS-D-17-0014.1), 2018.
- 1711
1712 Warren, J. L., and Zolensky, M. E., Collection and curation of interplanetary dust particles
1713 recovered from the stratosphere by NASA, In: *Analysis of Interplanetary Dust*, American



- 1714 Institute of Physics, M. Zolensk, T., Wilson, F. Rietmeijer, G. Flynn eds., New York, 245-253,
1715 1994.
1716
1717 Weigel, R., Volk, C. M., Kandler, K., Hösen, E., Günther, G., Vogel, B., Groß, J.-U., Khaykin, S.,
1718 Belyaev, G. V., and Borrmann, S., Enhancements of the refractory submicron aerosol fraction
1719 in the Arctic polar vortex: feature or exception?, *Atmos. Chem. Phys.*, 14, 12319–12342,
1720 2014.
1721
1722 Yu P., Toon O. B., Neely R. R., Martinsson B. G., and Brenninkmeijer C. A., Composition and
1723 physical properties of the Asian tropopause aerosol layer and the North American
1724 tropospheric aerosol layer, *Geophys. Res. Lett.*, 42, 2540–2546, 2015.
1725
1726 Zuev, V.V., Zueva, N.E., Koutsenogii, P.K. and Savelyeva, E.S., Volcanogenic nanosized carbon
1727 aerosol in the stratosphere, *Chemistry for sustainable development*, 22, 81-86, 2014.
1728
1729 Zuev, V.V., Zueva, N.E. and Savelyeva, E.S., Temperature and ozone anomalies as indicators
1730 of volcanic soot in the stratosphere, *Atmospheric and oceanic optics*, 28(1), 100-106, doi:
1731 10.1134/S1024856015010169, 2015.
1732